ORNL/TM-10975

OAK RIDGE NATIONAL LABORATORY

MARTIN MARIETTA

Shield Optimization Program, Part IV: Effects of Neutron and Gamma-Ray Radiations from Nuclear Weapons on SDI Weapon Platforms

M. S. Smith
J. O. Johnson
T. A. Gabriel
J. M. Barnes
J. D. Drischler
R. T. Santoro

OAK RIDGE NATIONAL LABORATORY
CENTRAL RESEARCH LIBRARY
CIRCULATION SECTION
4500N ROOM 175
LIBRARY LOAN COPY
DO NOT TRANSFER TO ANOTHER PERSON
If you wish someone else to see this report, send in name with report and the library will arrange a loan.

OPERATED BY
MARTIN MARIETTA ENERGY SYSTEMS, INC.
FOR THE UNITED STATES
DEPARTMENT OF ENERGY

Printed in the United States of America. Available from
National Technical Information Service
U.S. Department of Commerce
5285 Port Royal Road, Springfield, Virginia 22161
NTIS price codes—Printed Copy: A04; Microfiche A01

This report was prepared as an account of work sponsored by an agency of the United States Government. Neither the United States Government nor any agency thereof, nor any of their employees, makes any warranty, express or implied, or assumes any legal liability or responsibility for the accuracy, completeness, or usefulness of any information, apparatus, product, or process disclosed, or represents that its use would not infringe privately owned rights. Reference herein to any specific commercial product, process, or service by trade name, trademark, manufacturer, or otherwise, does not necessarily constitute or imply its endorsement, recommendation, or favoring by the United States Government or any agency thereof. The views and opinions of authors expressed herein do not necessarily state or reflect those of the United States Government or any agency thereof.

ORNL/TM-10975

Engineering Physics and Mathematics Division

Shield Optimization Program, Part IV: Effects of Neutron and Gamma-Ray Radiations from Nuclear Weapons on SDI Weapon Platforms

M. S. Smith, J. O. Johnson, T. A. Gabriel,
J. M. Barnes,* J. D. Drischler, and R. T. Santoro

Date Published - March 1989

*Computing and Telecommunications Division

Prepared by the
OAK RIDGE NATIONAL LABORATORY
Oak Ridge, Tennessee 37831
operated by
MARTIN MARIETTA ENERGY SYSTEMS, INC.
for the
U.S. DEPARTMENT OF ENERGY
under contract DE-AC05-84OR21400

MARTIN MARIETTA ENERGY SYSTEMS LIBRARIES

3 4456 0289964 7

PREFACE

The research reported here was performed for the Air Force Weapons Laboratory (AFWL) in support of the Strategic Defense Initiative Survivability Program.

The natural and man-made radiation environments of space pose significant potential threats to space deployed SDI systems. The data reported here are the results of an initial study to characterize the radiation induced damage to silicon based electronic components onboard a Space Based Interceptor (SBI) weapon platform due to neutrons and gamma rays emanating from a nuclear weapon detonation in space. The calculations performed in this study were carried out using three-dimensional radiation transport methods and an Oak Ridge National Laboratory (ORNL) conceptual model of a representative SBI weapon platform architecture.

CONTENTS

ABSTRACT xi
1. INTRODUCTION 1
1.1 SBI PLATFORM GEOMETRY 1
1.2 NUCLEAR WEAPON EFFECTS: NEUTRONS AND GAMMA RAYS 2
2. SOURCE SPECTRA 3
3. RADIATION EFFECTS ANALYSIS 4
4. RESULTS AND DISCUSSION 5
5. CONCLUSIONS 7
6. ACKNOWLEDGMENTS 8
REFERENCES 38

LIST OF FIGURES

Figure		Page
1	Calculational Model of the Space Based Interceptor Weapon Platform (a), with Interior Views Showing Launch Tube-Fuel Tanks Cluster (b), and the Central C^3 Bay (c)	31
2	Kinetic Kill Vehicle (a) and Exploded View of SBI Weapon Platform Showing KKVs Inside Launch Tubes (b)	32
3	DABL Unclassified Neutron Source Spectra	33
4	Normalized Fission Neutron Source Spectra	34
5	Schematic diagram of the Space Based Interceptor Weapon Platform Command, Control, Communications (C^3) Bay detailing the detector region numbering system used in the radiation transport analysis	35
6	Schematic diagram of the Space Based Interceptor Weapon Platform detailing the kinetic kill vehicle and fuel tank numbering system used in the radiation transport analysis	36
7	Schematic diagram of the Space Based Interceptor Weapon Platform depicting directions of incident nuclear weapon source spectra	37

LIST OF TABLES

Table		Page
1	46 Energy Group Neutron Source Spectra	9
2	23 Energy Group Gamma Ray Source Spectrum	10
3	The Detector Regions Implemented in the Radiation Transport Analysis Routines	11
4	Neutron and Gamma Dose Levels in the SBI Platform from the Deuterium–Tritium Fusion Source Positioned Directly Above the Platform Body	13
5	Neutron and Gamma Dose Levels in the SBI Platform from the Deuterium–Tritium Fusion Source Positioned Directly Above the Solar Panels	15
6	Neutron and Gamma Dose Levels in the SBI Platform from the Deuterium–Tritium Fusion Source Positioned Directly in Front of the Platform Body	17
7	Neutron and Gamma Dose Levels in the SBI Platform from the Deuterium–Tritium Fusion Source Positioned Directly in Front of and Above the Platform Body	19
8	Neutron and Gamma Dose Levels in the SBI Platform from the Fission Sources Positioned Directly Above the Platform Body	21
9	Neutron and Gamma Dose Levels in the SBI Platform from the Fission Sources Positioned Directly Above the Solar Panels	23
10	Neutron and Gamma Dose Levels in the SBI Platform from the Fission Sources Positioned Directly in Front of the Platform Body	25
11	Neutron and Gamma Dose Levels in the SBI Platform from the Fission Sources Positioned Directly in Front of and Above the Platform Body	27
12	Neutron Damage Dose Levels in Silicon Components from the Fusion Source for all Three Scenarios	29
13	Neutron Damage Dose Levels in Silicon Components from the ^{235}U Fission Source for all Three Scenarios	30

ABSTRACT

Initial studies have been completed to estimate the radiation induced damage in silicon based electronic components onboard a representative Space Based Interceptor (SBI) weapon platform. The SBI weapon platform model used in the studies represents the author's concept of such a system. The analysis was completed for neutrons and gamma rays emanating from a nuclear weapon detonation in space.

Results indicate dose levels to the sensitive components within the SBI weapon platform may exceed design limits if the weapon is detonated within a critical radius. For example, a 1962 Starfish detonation at a distance of 91.4 km from the SBI weapon platform generates a total dose in the central instrument bay of 964 rads(Si). The dose rate, $\dot{\gamma}$, assuming a 40 nsec deposition time, is 1×10^{10} rads(Si)/sec. All of the calculations were carried out for an unshielded SBI weapon platform to determine the radiation levels for which shielding must be designed to ensure survivability of the electronic systems.

1. INTRODUCTION

Electronic equipment, including modern integrated circuits, may undergo alteration of the electrical properties of the active components when exposed to various space radiation environments. These natural and man–made radiation environments include Van Allen belt protons and electrons; galactic and solar flare protons; neutrons, gamma rays, and X–rays from fission and fusion weapons; and directed neutral particle beams and lasers. The changes in the electrical characteristics can result in degradation of circuit performance or device failure. Furthermore, in a pulsed radiation environment, radiation induced photo currents can lead to transient circuit upsets.[1]

The objective of this study is to assess the dose levels within a generic Space Based Interceptor (SBI) carrier vehicle resulting from incident neutrons and gamma–rays generated by the detonation of a nuclear weapon. This study is part of a larger effort to evaluate the survivability of SDI space assets against nuclear and neutral particle beam weapon effects and natural space environments.[2–6]

To perform this extended analysis, a three dimensional ORNL computer model of a SBI platform was devised to estimate the effects of natural and nuclear weapon radiation on the external surfaces and materials and on the internal components. The external surfaces include the platform structure, kinetic energy and laser weapon shields, solar panels, antenna, etc. The internal components include electronic modules and circuits, sensors, interceptors, fuel, etc. Design details not relevant to the dose calculations have been omitted or purposely neglected in order to optimize the computational effort. A brief discussion of the SBI platform geometry will be provided in this section. Complete details, including the combinatorial geometry input, can be found in Reference 3. The remaining sections of this report cover the radiation sources employed, Section 2, the method of analysis, Section 3, presentation of results, Section 4, and conclusions in Section 5.

1.1 SBI PLATFORM GEOMETRY

The SBI weapon platform used in this study represents the author's concept of such a system and is not that proposed for deployment by the Strategic Defense Initiative Organization (SDIO). The platform was "designed" on the basis of space weapon system requirements eluded to in the Defense Acquisition Board documentation on SDI space weapon–sensor architecture requirements. Design guidance was also taken from briefings by other institutions also involved in weapon platform studies. In developing the platform representation shown in Figure 1, every effort has been made to protect proprietary information and configurations.

The ORNL weapon platform is a cylindrical shell comprised of two interceptor–fuel tank modules connected by a command, control, and communications bay. Each module contains five interceptor–launch tube assemblies and four fuel tanks. A cut-away view of the interior of the platform is provided in Figure 1b. Shown in this figure are the locations of the interceptor-launch tube assemblies and the fuel tanks, located on the same radius as the KKV launch tubes between the interceptors. The fuel is intended for maneuvering the platform to avoid collisions with space debris, evading enemy kill vehicles, and for positioning the platform during an engagement.

Power is supplied to the platform by solar panels shown in the deployed position in Figure 1a. A single antenna is shown, but it is recognized that other antennae and sensors may also exist on an actual platform design. A laser weapon shield covers the earth–exposed surfaces for protection against illumination by ground based laser weapons.

Figure 1c shows the command, control, and communications bay. The electronic circuits are housed in two concentric ring assemblies. At the center of the module is a "critical components" box. The cylindrical ring assemblies and the box are thin walled hollow assemblies that can be filled with detailed models of electronic circuitry or homogenized materials representative of those comprising the electronic packages. The electronics bay is also designed for the addition of shielding should it be necessary to further minimize the effects of radiation.

Figure 2a shows the details of an interceptor. Ten identical interceptors are modeled in their appropriate locations inside the platform. The principal components of each kill vehicle include the warhead, sensors, fuel tank, and rocket motor. The body of the interceptor will contain appropriate shielding (hardening) to protect the interceptor guidance system from exposure to weapon radiation outside of the platform during engagement. Two interceptors are positioned in their launch tubes in Figure 2b.

1.2 NUCLEAR WEAPON EFFECTS: NEUTRONS AND GAMMA RAYS

This paper describes the methodology and results of the effort to characterize the effect of incident neutrons and gamma rays on the ORNL model of the SBI platform. In particular, dose levels in the silicon components and fuel have been computed to quantify the damage sustained by the craft due to a nearby weapons burst. In addition, the neutron displacement damage dose has been calculated for the silicon components.

2. SOURCE SPECTRA

Source spectra employed in this study include a deuterium–tritium fusion reaction spectrum, a pure ^{235}U fission spectrum, and prompt fission gamma ray spectrum. The fusion and gamma ray spectra are unclassified and were taken from the 69 energy group Defense Applications Broad Group Library (DABL),[7] as were all cross sections employed in this study. The ^{235}U fission spectrum was taken to be

$$\chi(E) \propto e^{-E} \cdot \sinh\sqrt{2E},$$

i.e., a Watt spectrum.[8] These data are generic and can be used with appropriate weighting factors to describe actual weapons spectra.

Although DABL includes unclassified spectra for thermonuclear and tactical fission weapons, such spectra were not employed in this study. Due to the relative hardness of the ^{235}U fission spectrum as compared to the weapon spectra, the ^{235}U fission spectrum is more stressing than the fission components of the weapon spectra. The Watt spectrum is widely available, and more suitable for comparison calculations. For these reasons, the DABL weapon spectra were not utilized.

Tables 1 and 2 list the neutron and gamma ray spectra used in this study. The DABL neutron spectra are plotted in Figure 3 and Figure 4 shows the comparison between the unclassified tactical weapon spectrum and the ^{235}U fission spectrum.

3. RADIATION EFFECTS ANALYSIS

The MORSE (Multigroup Oak Ridge Stochastic Experiment)[9] code was used to perform all calculations in this study. The MORSE code is a multipurpose neutron and gamma–ray transport Monte Carlo code. Its features include the ability to treat the transport of either neutrons or gamma–rays or a coupled neutron and secondary gamma–ray problem, the incorporation of multigroup cross sections, and a three dimensional combinatorial geometry package.

The analysis routine used in the MORSE code calculates the dose to those areas of the platform which may be significantly affected by the incident radiation, *i.e.*, the electronic components. Neutron and gamma ray fluxes were obtained from particle track lengths calculated in each region of interest. These track lengths were then folded with their respective kerma factors from the DABL[7] data. To accommodate directional source spectra, such as that from a nuclear detonation, 68 different "detector" regions have been identified. The term "detector" is used to describe a component or volume for which results are being tabulated. In particular, the Command, Control, Communications (C^3) Bay contains 15 detector regions (see Figure 5). These include the critical electronic component box in the center of the C^3 Bay, six angular segments for the inner electronic bay ring, and eight angular segments for the outer electronic bay ring. The angular segmenting of the electronic bay rings will identify variations in the dose due to the inherent shielding designed into the platform. This will be important when considering directional source spectra.

There are ten kinetic kill vehicles (KKVs) onboard the platform, each with a computer and sensor region. For the same reasons stated above, each computer or sensor has been identified as a separate detector region. The solar panels have been modeled as two separate detector regions. Furthermore, since the solar panels are on the exterior of the platform and in direct contact with the incident radiation, each panel has been subdivided into five additional detector regions to calculate dose profiles in the solar panels and identify potential surface phenomenology, i.e. blowoff, melting, etc. Each fuel tank in the platform and KKV is also a detector region. Finally, the Boost Surveillance and Tracking System (BSTS), Space Surveillance and Tracking System (SSTS) antenna has been modeled as five separate detector regions. Table 3 lists the detector regions implemented in the analysis module. Figure 6 shows the relative locations for some of these detector regions.

To accommodate the directional source spectra incident on the SBI platform from a nuclear detonation, three scenarios will be considered in the analysis. The first scenario will model the nuclear detonation directly above the SBI platform, the second scenario will model the nuclear detonation directly in front of the SBI platform, and the third scenario will model the nuclear detonation incident on the top and front of the platform at a 45 degree angle. The nuclear weapon detonation will be modeled such that the incident radiation spectra will be monodirectional. Figure 7 illustrates the incident directions for the three scenarios.

4. RESULTS AND DISCUSSION

Dose levels in the ORNL model of an SBI platform from three nuclear weapon spectra: a deuterium–tritium fusion reaction, ^{235}U fission, and prompt fission gamma rays, each with three illumination scenarios, have been calculated using the MORSE Monte Carlo code.

The MORSE code results were obtained from 500,000 particle histories (100 batches of 5000 particles each) yielding excellent fractional standard deviations (fsd) in the regions of interest. All calculations have been normalized to a one kiloton output of neutrons and gamma–rays, assuming 100% efficiency. This assumption results in 1.88×10^{23} prompt fission neutrons and 1.06×10^{24} prompt fission gamma–rays, or 1.49×10^{24} fusion neutrons, per kiloton of yield. The tabulated data is in units of rads(material)$\cdot m^2$/kTon. The dose received by a particular component can be quickly assessed by multiplying by the device yield and dividing by the square of the separation distance. Note that the factor of 4π has already been included in the tabulated data. An actual weapon spectrum may be a combination of fusion and fission components, which can be modeled using the spectra in this report. The gamma–ray contribution from the coupled sources may vary between approximately 33% (pure fusion) and approximately 95% (pure fission).

There are ten tables of results listing dose levels for each of the 68 detector regions identified in Table 3. Tables 4 through 7 consider the deuterium–tritium fusion source and Tables 8 through 11 examine the fission sources. Tables 12 and 13 list the neutron displacement damage dose levels for the fusion and fission sources, respectively. For each source spectrum, the following illumination scenarios apply: top, platform body only; top, solar panels only; front, platform body only; and front with an angle of elevation of 45°, platform body only. This methodology was chosen because the solar panels may or may not be deployed during device detonation. The dose values for the solar panels (detectors 36 through 45) for the top, platform body only illumination scenario are for secondary particles only, and similarly for the platform body in the top, solar panel only illumination scenario. Consequently, the fsd values for these results may be high. For the neutron displacement damage results, only the silicon components are listed.

The total dose level in a component is a summation of the contributions from the primary and secondary particles. For example, a 100 kTon fission device detonated at 1 kilometer above the SBI platform (scenario 1) generates a total dose in the central instrument box of 26.5 krad(Si) from primary neutrons, primary gamma rays (prompt gamma rays), and secondary gamma rays. Although the solar panels were not irradiated directly in this example, significant doses are attained ($\approx$ 7.5 krad) due to secondary particle generation and scattering of primary particles.

The calculated maximum dose in the central instrument bay (detector 1 in Table 3) is 1.51×10^{10} rads(Si)$\cdot m^2$/kTon, using the third scenario, in front of the platform body and elevated to 45°, and the deuterium–tritium fusion source. In contrast, the dose in the central instrument box, for the same scenario, but using the fission sources is 2.03×10^9 rads(Si)$\cdot m^2$/kTon. Both values include doses from secondary particles. Greater dose levels (by a factor of 7) are calculated in the third scenario, because there is less internal shielding and, consequently, less attenuation of the primary particles.

Some interesting, but not unexpected, trends are shown by these results. For example, consider the deuterium–tritium fusion source with the frontal exposure. The highest silicon doses are in the forward KKV sensors (detectors 26 to 30). The doses in the aft sensors are smaller by a factor of 40, clearly showing the effects of internal shielding. In the instrument bay, the dose level in the central box is eight times smaller than levels in the inner ring, due to shielding by the central KKV. The outer instrument ring dose levels are also lower than those in the inner ring, because of KKV shielding.

The highest dose levels in this study were calculated for the platform fuel tanks (hydrazine) from the deuterium–tritium fusion source with the top, platform body only, illumination scenario. These values were in excess of 3×10^{11} rads(N_2H_4)$\cdot m^2$/kTon for the upper tanks. Hydrazine dose levels were calculated because of concerns of radiation–induced chemical degradation.

The neutron displacement damage dose levels in the silicon components are small compared to the total dose for the deuterium–tritium fusion source, even a factor of five below the dose from the secondary gamma rays. Similarly, displacement damage dose levels for the fission source are comparable to the secondary gamma dose levels. For both source types, neutron displacement damage contributes less than 5% to the total dose. The same trends apply as discussed above, displacement damage levels are much greater for the fusion source and the third scenario (12:00 o'clock high) produces the greatest doses.

These results are consistent with those obtained in the previous fiscal year. In FY87, using a simple 1D spherical platform with the KEW (Kinetic Energy Weapon) shield and similar source spectra, total dose levels were approximately an order of magnitude higher.[10] The decrease is partly due to the presence of structural components within the platform, in contrast to the void in the 1D spherical model.

5. CONCLUSIONS

An extensive study has been performed to characterize the dose levels in an ORNL computer model of a space weapons platform resulting from incident radiation from a nuclear detonation in the vicinity of the platform. Results have been tabulated in units of rads(material)$\cdot$m^2/kTon to facilitate device yield and separation distance comparisons. Time dependence has not been considered in this study. Other reports in this series examine the effects of natural radiation fields, pumped Van Allen belts, and X–rays.

Dose levels in the "critical components box" (detector 1) are greatest for the deuterium–tritium source incident from the front and angled upward at 45° (scenario 3). For this case, assuming a yield of 100 kTon, the source must be at least 12.3 km away to assure a dose level below 10 krad(Si) in the central instrument bay (detector 1). For a fission device of identical yield, the "keep–out" distance falls to 4.5 km. The smallest dose to this region is generated in the frontal scenario, where there is significant internal shielding from the central KKV.

If a deposition time of 40 nsec is coupled with the gamma ray dose levels associated with the above keep–out distances, dose rates ($\dot{\gamma}$) of 6.15×10^{10} rads(Si)/sec for the fusion source and 2.38×10^{11} for the fission source are obtained. Note that the $\dot{\gamma}$ value for the fission source includes both prompt and secondary gamma rays. Dose rates of these magnitudes are sufficient to cause transient upset, latchup, or burnout in semiconductor devices. To reduce the $\dot{\gamma}$ values in the central instrument bay to below 10^9 rads(Si)/sec, the keep–out distances would have to be increased to 96.4 km and 69.5 km for the fusion and fission sources, respectively.

The results in this paper can be normalized to X–ray surface loadings. If it is assumed that 75% of the energy from a detonation is in the form of X–rays, then device yields may be converted to surface loadings (using 10^{12} cal/kT). For example, the 1962 Starfish event had a yield of 1.4 MT, of which 1 MT was fission yield. At a distance of 91.4 km from the device, the surface loading is 1 cal/cm^2. Using this distance and yield, coupled with the source spectra employed in this report, total dose and dose rate can be calculated for the ORNL SBI model. The total dose in the central instrument bay (detector 1), considering the third scenario (worst case), is 964 rads(Si). The dose rate, $\dot{\gamma}$, is 1.0×10^{10} rads(Si)/sec. As was seen above, the limiting factor is the dose rate. If the surface loading is doubled, the separation distance decreases to 64.6 km, and the dose and dose rate increase by a factor of 2, also.

Electronic devices can be hardened to withstand high levels of neutron fluence and dose. Therefore, the gamma dose level and dose rate predominates in terms of electronic component shielding. An actual weapon spectrum may be a combination of fusion and fission components, which can be modeled using the spectra in this report. The gamma–ray contribution from the coupled sources may vary between approximately 33% (pure fusion) and approximately 95% (pure fission). By adding some high–Z material around the central instrument bay, significant reductions in gamma dose may be obtained. A future study will investigate the effects of shield materials on the dose levels in the central instrument bay.

6. ACKNOWLEDGMENTS

The authors wish to thank Mrs. Dawn C. Human for her significant efforts in typing this manuscript and for her assistance throughout this program.

Table 1
46 Energy Group Neutron Source Spectra

Group	Energy Range (eV)	D–T Fusion	^{235}U Fission
1	1.9640+07[a]– 1.6905+07	0.0	0.0
2	1.6905+07 — 1.4918+07	1.89–02	1.86–05
3	1.4918+07 — 1.4191+07	3.12–01	1.88–05
4	1.4191+07 — 1.3840+07	3.12–01	1.39–05
5	1.3840+07 — 1.2523+07	3.54–01	1.07–04
6	1.2523+07 — 1.2214+07	4.37–03	4.61–05
7	1.2214+07 — 1.1052+07	0.0	3.21–04
8	1.1052+07 — 1.0000+07	0.0	6.90–04
9	1.0000+07 — 9.0484+06	0.0	1.35–03
10	9.0484+06 — 8.1873+06	0.0	2.44–03
11	8.1873+06 — 7.4082+06	0.0	4.07–03
12	7.4082+06 — 6.3763+06	0.0	1.06–02
13	6.3763+06 — 4.9659+06	0.0	3.54–02
14	4.9659+06 — 4.7237+06	0.0	1.04–02
15	4.7237+06 — 4.0657+06	0.0	3.83–02
16	4.0657+06 — 3.0119+06	0.0	1.07–01
17	3.0119+06 — 2.3852+06	0.0	1.04–01
18	2.3852+06 — 2.3069+06	0.0	1.56–02
19	2.3069+06 — 1.8268+06	0.0	1.10–01
20	1.8268+06 — 1.4227+06	0.0	1.14–01
21	1.4227+06 — 1.1080+06	0.0	1.01–01
22	1.1080+06 — 9.6164+05	0.0	5.00–02
23	9.6164+05 — 8.2085+05	0.0	4.94–02
24	8.2085+05 — 7.4274+05	0.0	2.77–02
25	7.4274+05 — 6.3928+05	0.0	3.68–02
26	6.3928+05 — 5.5023+05	0.0	3.14–02
27	5.5023+05 — 3.6883+05	0.0	6.15–02
28	3.6883+05 — 2.4724+05	0.0	3.74–02
29	2.4724+05 — 1.5764+05	0.0	2.40–02
30	1.5764+05 — 1.1109+05	0.0	1.07–02
31	1.1109+05—5.2475+04	0.0	1.08–02
32	5.2475+04—3.4307+04	0.0	2.51–03
33	3.4307+04—2.4788+04	0.0	1.10–03
34	2.4788+04—2.1875+04	0.0	3.00–04
35	2.1875+04—1.0595+04	0.0	9.68–04
36	1.0595+04—3.3546+03	0.0	4.07–04
37	3.3546+03—1.2341+03	0.0	6.88–05
38	1.2341+03—5.8295+02	0.0	1.34–05
39	5.8295+02—2.7536+02	0.0	0.0
40	2.7536+02—1.0130+02	0.0	0.0
41	1.0130+02—2.9023+01	0.0	0.0
42	2.9023+01—1.0677+01	0.0	0.0
43	1.0677+01—3.0590+00	0.0	0.0
44	3.0590+00—1.1254+00	0.0	0.0
45	1.1254+00—4.1399–01	0.0	0.0
46	4.1399–01—1.0000–05	0.0	0.0

[a]Read as 1.9640×10^7.

Table 2

23 Energy Group Gamma Ray Source Spectrum

Group	Energy Range (eV)	Prompt Fission
1	2.00+07[a] — 1.40+07	0.0
2	1.40+07 — 1.20+07	8.25−06
3	1.20+07 — 1.00+07	8.25−06
4	1.00+07 — 8.00+06	1.34−04
5	8.00+06 — 7.00+06	3.02−04
6	7.00+06 — 6.00+06	9.08−04
7	6.00+06 — 5.00+06	2.73−03
8	5.00+06 — 4.00+06	8.19−03
9	4.00+06 — 3.00+06	2.46−02
10	3.00+06 — 2.50+06	2.70−02
11	2.50+06 — 2.00+06	4.69−02
12	2.00+06 — 1.50+06	8.12−02
13	1.50+06 — 1.00+06	1.43−01
14	1.00+06 — 7.00+05	1.32−01
15	7.00+05 — 4.50+05	1.50−01
16	4.50+05 — 3.00+05	1.11−01
17	3.00+05 — 1.50+05	1.31−01
18	1.50+05 — 1.00+05	4.79−02
19	1.00+05 — 7.00+04	3.01−02
20	7.00+04 — 4.50+04	2.58−02
21	4.50+04 — 3.00+04	1.58−02
22	3.00+04 — 2.00+04	1.07−02
23	2.00+04 — 1.00+04	1.08−02

[a]Read as 2.00×10^7.

Table 3

The Detector Regions Implemented in the Radiation Transport Analysis Routines

SBI Platform Component	Detector Region
C^3 Bay Critical Components Central Instrument Box[a]	1
C^3 Bay Inner Instrument Ring[a]	
0 to 60 Degree Segment	2
60 to 120 Degree Segment	3
120 to 180 Degree Segment	4
180 to 240 Degree Segment	5
240 to 300 Degree Segment	6
300 to 360 Degree Segment	7
C^3 Bay Outer Instrument Ring[a]	
0 to 45 Degree Segment	8
45 to 90 Degree Segment	9
90 to 135 Degree Segment	10
135 to 180 Degree Segment	11
180 to 225 Degree Segment	12
225 to 270 Degree Segment	13
270 to 315 Degree Segment	14
315 to 360 Degree Segment	15
Kinetic Kill Vehicle Computers[a]	
KKV Number 1	16
KKV Number 2	17
KKV Number 3	18
KKV Number 4	19
KKV Number 5	20
KKV Number 6	21
KKV Number 7	22
KKV Number 8	23
KKV Number 9	24
KKV Number 10	25
Kinetic Kill Vehicle Sensors[a]	
KKV Number 1	26
KKV Number 2	27
KKV Number 3	28
KKV Number 4	29
KKV Number 5	30
KKV Number 6	31
KKV Number 7	32
KKV Number 8	33
KKV Number 9	34
KKV Number 10	35

Table 3 (Continued)

SBI Platform Component	Detector Region
Right Solar Panel[b]	
Inner 0.5 cm Thick Shell	36
Next 0.5 cm Thick Shell	37
Next 0.5 cm Thick Shell	38
Next 0.5 cm Thick Shell	39
Outer 0.5 cm Thick Shell	40
Left Solar Panel[b]	
Inner 0.5 cm Thick Shell	41
Next 0.5 cm Thick Shell	42
Next 0.5 cm Thick Shell	43
Next 0.5 cm Thick Shell	44
Outer 0.5 cm Thick Shell	45
BSTS, SSTS Antenna[a]	
Inner 1.0 cm Thick Shell	46
Next 1.0 cm Thick Shell	47
Next 1.0 cm Thick Shell	48
Next 1.0 cm Thick Shell	49
Outer 1.0 cm Thick Shell	50
Kinetic Kill Vehicle Rocket Fuel Tanks[c]	
KKV Number 1	51
KKV Number 2	52
KKV Number 3	53
KKV Number 4	54
KKV Number 5	55
KKV Number 6	56
KKV Number 7	57
KKV Number 8	58
KKV Number 9	59
KKV Number 10	60
SBI Weapon Platform Rocket Fuel Tanks[d]	
SBI Tank Number 1	61
SBI Tank Number 2	62
SBI Tank Number 3	63
SBI Tank Number 4	64
SBI Tank Number 5	65
SBI Tank Number 6	66
SBI Tank Number 7	67
SBI Tank Number 8	68

[a]Silicon at 20% theoretical density.
[b]90% beryllium/10% silicon at 50% theoretical density.
[c]Hydrazine at 25% theoretical density.
[d]Hydrazine at 100% theoretical density.

Table 4

Neutron and Gamma Dose Levels in the SBI Platform from the Deuterium–Tritium Fusion Source Positioned Directly Above the Platform Body (rads·m^2/kTon)[a]

	Neutron	Secondary Gamma
1	1.398+09[b] ± 0.037[c]	7.436+08 ± 0.074
2	1.702+09 ± 0.030	8.011+08 ± 0.071
3	1.506+09 ± 0.026	7.780+08 ± 0.079
4	1.247+09 ± 0.038	8.463+08 ± 0.070
5	2.111+09 ± 0.031	8.615+08 ± 0.078
6	1.906+09 ± 0.023	1.034+09 ± 0.064
7	1.556+09 ± 0.032	1.006+09 ± 0.064
8	2.164+09 ± 0.034	7.874+08 ± 0.062
9	1.171+09 ± 0.026	5.741+08 ± 0.063
10	1.152+09 ± 0.027	6.425+08 ± 0.065
11	1.237+09 ± 0.035	7.590+08 ± 0.065
12	3.014+09 ± 0.027	9.871+08 ± 0.058
13	2.368+09 ± 0.022	1.014+09 ± 0.050
14	2.287+09 ± 0.018	1.003+09 ± 0.060
15	2.123+09 ± 0.027	9.654+08 ± 0.058
16	2.009+09 ± 0.024	8.656+08 ± 0.063
17	1.404+09 ± 0.029	6.093+08 ± 0.091
18	2.699+09 ± 0.022	9.217+08 ± 0.063
19	2.180+09 ± 0.024	8.313+08 ± 0.071
20	2.207+09 ± 0.023	7.116+08 ± 0.067
21	2.046+09 ± 0.029	8.103+08 ± 0.070
22	1.427+09 ± 0.031	6.168+08 ± 0.067
23	2.684+09 ± 0.023	9.641+08 ± 0.061
24	2.209+09 ± 0.024	8.687+08 ± 0.062
25	2.219+09 ± 0.028	8.103+08 ± 0.064
26	1.777+09 ± 0.023	6.882+08 ± 0.054
27	1.204+09 ± 0.026	4.830+08 ± 0.068
28	2.524+09 ± 0.020	9.416+08 ± 0.062
29	1.876+09 ± 0.022	7.384+08 ± 0.050
30	1.928+09 ± 0.023	7.430+08 ± 0.067
31	1.752+09 ± 0.020	7.276+08 ± 0.052
32	1.120+09 ± 0.024	5.152+08 ± 0.055
33	2.498+09 ± 0.021	7.977+08 ± 0.051
34	2.013+09 ± 0.022	7.025+08 ± 0.054

Table 4 (Continued)

	Neutron	Secondary Gamma
35	1.913+09 ± 0.021	6.395+08 ± 0.052
36	2.454+07 ± 0.057	1.078+08 ± 0.044
37	1.114+07 ± 0.074	2.577+07 ± 0.075
38	9.606+06 ± 0.081	2.639+07 ± 0.122
39	1.019+07 ± 0.062	1.513+07 ± 0.064
40	4.999+06 ± 0.070	9.779+06 ± 0.072
41	2.648+07 ± 0.058	1.121+08 ± 0.050
42	1.160+07 ± 0.079	2.477+07 ± 0.078
43	1.162+07 ± 0.069	2.160+07 ± 0.077
44	9.750+06 ± 0.065	2.131+07 ± 0.085
45	5.862+06 ± 0.070	9.541+06 ± 0.092
46	1.283+10 ± 0.012	1.347+09 ± 0.077
47	1.302+09 ± 0.027	8.713+08 ± 0.107
48	1.085+09 ± 0.034	5.932+08 ± 0.094
49	9.228+08 ± 0.029	4.536+08 ± 0.115
50	7.041+08 ± 0.034	2.018+08 ± 0.134
51	5.180+10 ± 0.017	1.308+09 ± 0.031
52	2.845+10 ± 0.019	8.188+08 ± 0.043
53	9.256+10 ± 0.014	1.484+09 ± 0.032
54	7.242+10 ± 0.015	1.206+09 ± 0.032
55	7.485+10 ± 0.014	1.150+09 ± 0.033
56	5.281+10 ± 0.017	1.314+09 ± 0.035
57	2.978+10 ± 0.019	8.141+08 ± 0.042
58	9.553+10 ± 0.014	1.545+09 ± 0.027
59	7.634+10 ± 0.015	1.264+09 ± 0.032
60	7.325+10 ± 0.015	1.231+09 ± 0.033
61	9.313+10 ± 0.016	3.426+09 ± 0.028
62	9.247+10 ± 0.017	3.329+09 ± 0.030
63	3.234+11 ± 0.008	6.197+09 ± 0.018
64	3.277+11 ± 0.009	6.457+09 ± 0.018
65	8.985+10 ± 0.018	3.240+09 ± 0.024
66	9.360+10 ± 0.016	3.383+09 ± 0.028
67	3.243+11 ± 0.009	6.331+09 ± 0.015
68	3.278+11 ± 0.008	6.296+09 ± 0.018

[a]A factor of 4π has already been included in these values.
[b]Read as 1.398×10^9.
[c]Fractional Standard Deviation.

Table 5

Neutron and Gamma Dose Levels in the SBI Platform from the Deuterium–Tritium Fusion Source Positioned Directly Above the Solar Panels (rads·m^2/kTon)[a]

	Neutron	Secondary Gamma
1	8.032+06[b] ± 0.530[c]	1.523+07 ± 0.401
2	9.629+06 ± 0.381	1.231+07 ± 0.264
3	1.235+07 ± 0.407	1.589+07 ± 0.305
4	1.322+07 ± 0.361	2.688+07 ± 0.414
5	1.564+07 ± 0.297	1.562+07 ± 0.433
6	2.096+07 ± 0.303	2.141+07 ± 0.265
7	1.175+07 ± 0.313	3.503+07 ± 0.380
8	2.180+07 ± 0.257	1.547+07 ± 0.214
9	3.425+07 ± 0.303	1.172+07 ± 0.346
10	3.432+07 ± 0.277	1.694+07 ± 0.499
11	2.210+07 ± 0.223	2.799+07 ± 0.275
12	1.772+07 ± 0.261	1.835+07 ± 0.203
13	1.033+07 ± 0.418	8.380+06 ± 0.236
14	2.582+07 ± 0.282	3.230+07 ± 0.482
15	2.060+07 ± 0.175	1.890+07 ± 0.214
16	5.140+06 ± 0.539	6.419+06 ± 0.304
17	1.059+07 ± 0.358	9.037+06 ± 0.488
18	2.407+06 ± 0.294	9.172+06 ± 0.288
19	3.996+06 ± 0.432	7.493+06 ± 0.336
20	1.032+07 ± 0.335	1.352+07 ± 0.316
21	3.745+06 ± 0.404	1.118+07 ± 0.348
22	4.590+06 ± 0.527	2.548+07 ± 0.356
23	7.158+06 ± 0.437	7.688+06 ± 0.254
24	7.731+06 ± 0.422	1.151+07 ± 0.282
25	1.161+07 ± 0.306	1.311+07 ± 0.256
26	5.647+06 ± 0.373	7.285+06 ± 0.376
27	3.831+06 ± 0.343	1.086+07 ± 0.290
28	6.811+06 ± 0.345	7.972+06 ± 0.250
29	1.131+07 ± 0.330	1.392+07 ± 0.333
30	8.115+06 ± 0.350	7.882+06 ± 0.401
31	7.958+06 ± 0.389	1.209+07 ± 0.289
32	7.930+06 ± 0.311	1.343+07 ± 0.287
33	8.819+06 ± 0.299	4.087+06 ± 0.328
34	9.775+06 ± 0.347	9.827+06 ± 0.284

Table 5 (Continued)

	Neutron	Secondary Gamma
35	9.118+06 ± 0.350	4.228+06 ± 0.227
36	5.404+09 ± 0.004	7.195+07 ± 0.033
37	7.811+08 ± 0.009	6.255+07 ± 0.042
38	6.165+08 ± 0.010	4.672+07 ± 0.035
39	4.331+08 ± 0.010	3.340+07 ± 0.035
40	2.007+08 ± 0.013	1.344+07 ± 0.056
41	5.415+09 ± 0.003	7.008+07 ± 0.039
42	7.551+08 ± 0.009	6.162+07 ± 0.037
43	6.225+08 ± 0.010	4.518+07 ± 0.044
44	4.295+08 ± 0.009	3.606+07 ± 0.043
45	2.022+08 ± 0.015	1.333+07 ± 0.047
46	1.508+08 ± 0.139	5.423+07 ± 0.189
47	2.653+07 ± 0.186	2.128+07 ± 0.285
48	1.977+07 ± 0.190	1.489+07 ± 0.573
49	1.494+07 ± 0.184	7.100+06 ± 0.252
50	7.178+06 ± 0.234	2.012+06 ± 0.281
51	5.716+08 ± 0.180	2.931+07 ± 0.221
52	8.054+08 ± 0.158	3.522+07 ± 0.169
53	7.603+08 ± 0.153	2.844+07 ± 0.172
54	1.278+09 ± 0.132	3.468+07 ± 0.198
55	9.089+08 ± 0.160	3.969+07 ± 0.210
56	7.034+08 ± 0.176	2.504+07 ± 0.194
57	9.663+08 ± 0.158	4.534+07 ± 0.247
58	7.005+08 ± 0.157	2.641+07 ± 0.183
59	1.086+09 ± 0.137	2.909+07 ± 0.173
60	9.188+08 ± 0.181	3.002+07 ± 0.260
61	3.229+09 ± 0.108	1.277+08 ± 0.108
62	3.056+09 ± 0.096	1.458+08 ± 0.103
63	4.316+09 ± 0.091	1.471+08 ± 0.106
64	3.892+09 ± 0.090	1.393+08 ± 0.094
65	3.093+09 ± 0.123	1.732+08 ± 0.175
66	3.197+09 ± 0.109	1.826+08 ± 0.161
67	4.693+09 ± 0.087	1.542+08 ± 0.103
68	4.370+09 ± 0.088	1.411+08 ± 0.088

[a]A factor of 4π has already been included in these values.
[b]Read as 8.032×10^6.
[c]Fractional Standard Deviation.

Table 6

Neutron and Gamma Dose Levels in the SBI Platform from the Deuterium–Tritium Fusion Source Positioned Directly in Front of the Platform Body (rads·m^2/kTon)[a]

	Neutron	Secondary Gamma
1	2.899+08[b] ± 0.037[c]	3.340+08 ± 0.071
2	2.314+09 ± 0.020	6.203+08 ± 0.052
3	2.128+09 ± 0.017	5.828+08 ± 0.049
4	2.397+09 ± 0.018	6.041+08 ± 0.054
5	2.371+09 ± 0.016	6.276+08 ± 0.057
6	2.188+09 ± 0.021	5.705+08 ± 0.056
7	2.328+09 ± 0.021	5.968+08 ± 0.050
8	8.454+08 ± 0.023	3.631+08 ± 0.052
9	9.005+08 ± 0.021	3.569+08 ± 0.049
10	8.540+08 ± 0.022	3.641+08 ± 0.054
11	8.560+08 ± 0.022	3.667+08 ± 0.056
12	8.499+08 ± 0.024	3.635+08 ± 0.052
13	8.921+08 ± 0.025	3.597+08 ± 0.057
14	8.826+08 ± 0.025	3.788+08 ± 0.054
15	8.576+08 ± 0.021	3.498+08 ± 0.055
16	1.625+09 ± 0.021	5.848+08 ± 0.049
17	1.587+09 ± 0.019	4.729+08 ± 0.050
18	1.557+09 ± 0.019	5.175+08 ± 0.058
19	1.586+09 ± 0.022	4.472+08 ± 0.057
20	1.603+09 ± 0.022	4.687+08 ± 0.048
21	9.016+07 ± 0.064	6.070+07 ± 0.103
22	6.588+07 ± 0.085	4.606+07 ± 0.133
23	7.481+07 ± 0.065	4.894+07 ± 0.153
24	6.526+07 ± 0.088	4.005+07 ± 0.143
25	6.622+07 ± 0.075	4.508+07 ± 0.159
26	2.497+09 ± 0.013	7.113+08 ± 0.037
27	2.518+09 ± 0.012	6.248+08 ± 0.036
28	2.497+09 ± 0.011	6.317+08 ± 0.034
29	2.457+09 ± 0.011	6.092+08 ± 0.041
30	2.506+09 ± 0.012	6.447+08 ± 0.039
31	8.186+07 ± 0.050	3.758+07 ± 0.088
32	5.811+07 ± 0.064	3.821+07 ± 0.104
33	6.607+07 ± 0.063	3.197+07 ± 0.120
34	6.350+07 ± 0.067	3.432+07 ± 0.124

Table 6 (Continued)

	Neutron	Secondary Gamma
35	6.440+07 ± 0.063	3.880+07 ± 0.131
36	5.434+06 ± 0.077	2.245+07 ± 0.063
37	3.071+06 ± 0.101	6.100+06 ± 0.117
38	3.256+06 ± 0.069	5.748+06 ± 0.103
39	2.833+06 ± 0.080	5.330+06 ± 0.138
40	2.254+06 ± 0.074	2.678+06 ± 0.100
41	5.233+06 ± 0.080	2.320+07 ± 0.064
42	2.494+06 ± 0.094	6.707+06 ± 0.093
43	3.125+06 ± 0.099	5.398+06 ± 0.098
44	3.126+06 ± 0.096	3.837+06 ± 0.083
45	2.334+06 ± 0.074	2.246+06 ± 0.092
46	9.155+07 ± 0.073	1.331+08 ± 0.084
47	1.705+07 ± 0.148	3.409+07 ± 0.185
48	1.291+07 ± 0.136	3.063+07 ± 0.154
49	1.117+07 ± 0.148	1.793+07 ± 0.150
50	4.957+06 ± 0.157	8.987+06 ± 0.145
51	5.416+10 ± 0.010	6.833+08 ± 0.026
52	5.187+10 ± 0.011	5.083+08 ± 0.026
53	5.163+10 ± 0.012	5.216+08 ± 0.028
54	5.115+10 ± 0.013	5.033+08 ± 0.026
55	5.206+10 ± 0.011	5.164+08 ± 0.027
56	1.180+10 ± 0.021	2.043+08 ± 0.047
57	9.503+09 ± 0.022	1.511+08 ± 0.043
58	9.252+09 ± 0.025	1.373+08 ± 0.056
59	9.393+09 ± 0.026	1.463+08 ± 0.051
60	9.304+09 ± 0.024	1.543+08 ± 0.048
61	4.947+10 ± 0.016	1.787+09 ± 0.021
62	4.973+10 ± 0.016	1.727+09 ± 0.021
63	4.914+10 ± 0.017	1.764+09 ± 0.021
64	5.000+10 ± 0.015	1.800+09 ± 0.023
65	9.506+09 ± 0.033	4.762+08 ± 0.038
66	8.825+09 ± 0.028	4.772+08 ± 0.052
67	9.208+09 ± 0.030	4.932+08 ± 0.054
68	8.632+09 ± 0.032	4.604+08 ± 0.043

[a]A factor of 4π has already been included in these values.
[b]Read as 2.899×10^8.
[c]Fractional Standard Deviation.

Table 7

Neutron and Gamma Dose Levels in the SBI Platform from the Deuterium–Tritium Fusion Source Positioned Directly in Front of and Above the Platform Body (rads·m²/kTon)[a]

	Neutron	Secondary Gamma
1	1.135+10[b] ± 0.017[c]	3.718+09 ± 0.093
2	7.036+08 ± 0.047	7.269+08 ± 0.098
3	3.473+08 ± 0.055	5.060+08 ± 0.113
4	5.968+08 ± 0.044	6.450+08 ± 0.101
5	1.020+09 ± 0.039	8.171+08 ± 0.087
6	8.415+08 ± 0.033	9.584+08 ± 0.115
7	1.118+09 ± 0.043	7.450+08 ± 0.086
8	2.019+09 ± 0.024	7.607+08 ± 0.078
9	1.281+09 ± 0.026	4.628+08 ± 0.077
10	1.338+09 ± 0.029	5.509+08 ± 0.080
11	2.031+09 ± 0.028	6.863+08 ± 0.072
12	2.151+09 ± 0.028	6.254+08 ± 0.073
13	2.383+09 ± 0.018	7.517+08 ± 0.069
14	2.448+09 ± 0.020	7.595+08 ± 0.074
15	2.354+09 ± 0.025	7.441+08 ± 0.077
16	1.675+08 ± 0.083	2.026+08 ± 0.096
17	2.596+08 ± 0.065	2.161+08 ± 0.097
18	1.534+08 ± 0.069	2.227+08 ± 0.110
19	1.595+08 ± 0.086	2.596+08 ± 0.195
20	1.378+08 ± 0.083	2.154+08 ± 0.108
21	1.457+08 ± 0.090	2.199+08 ± 0.106
22	2.048+08 ± 0.078	1.725+08 ± 0.120
23	2.266+08 ± 0.073	2.515+08 ± 0.105
24	1.817+08 ± 0.081	2.197+08 ± 0.116
25	1.377+08 ± 0.076	1.604+08 ± 0.108
26	1.673+08 ± 0.072	1.863+08 ± 0.081
27	2.507+08 ± 0.048	2.056+08 ± 0.077
28	8.677+08 ± 0.027	3.418+08 ± 0.080
29	1.498+08 ± 0.067	2.109+08 ± 0.103
30	1.143+08 ± 0.072	1.742+08 ± 0.092
31	1.422+08 ± 0.064	1.789+08 ± 0.091
32	1.793+08 ± 0.072	1.709+08 ± 0.098
33	9.508+08 ± 0.029	2.776+08 ± 0.092
34	1.701+08 ± 0.064	2.196+08 ± 0.116

Table 7 (Continued)

	Neutron	Secondary Gamma
35	1.209+08 ± 0.059	1.555+08 ± 0.086
36	1.916+07 ± 0.059	5.615+07 ± 0.055
37	8.219+06 ± 0.080	1.217+07 ± 0.091
38	6.532+06 ± 0.082	1.233+07 ± 0.073
39	5.868+06 ± 0.070	9.838+06 ± 0.155
40	3.694+06 ± 0.072	4.518+06 ± 0.103
41	2.058+07 ± 0.055	5.675+07 ± 0.052
42	8.692+06 ± 0.085	1.373+07 ± 0.114
43	7.567+06 ± 0.081	1.297+07 ± 0.122
44	6.156+06 ± 0.073	1.012+07 ± 0.102
45	3.478+06 ± 0.076	4.970+06 ± 0.114
46	1.225+10 ± 0.012	1.009+09 ± 0.094
47	1.660+09 ± 0.029	6.590+08 ± 0.147
48	1.331+09 ± 0.032	6.168+08 ± 0.125
49	9.099+08 ± 0.028	4.531+08 ± 0.130
50	3.905+08 ± 0.035	1.711+08 ± 0.116
51	1.059+10 ± 0.038	4.514+08 ± 0.048
52	1.105+10 ± 0.035	4.152+08 ± 0.058
53	4.720+10 ± 0.018	5.193+08 ± 0.043
54	1.022+10 ± 0.035	4.427+08 ± 0.044
55	8.368+09 ± 0.037	3.725+08 ± 0.059
56	1.218+10 ± 0.030	5.295+08 ± 0.044
57	1.190+10 ± 0.032	4.181+08 ± 0.057
58	3.947+10 ± 0.018	5.534+08 ± 0.042
59	1.078+10 ± 0.035	4.375+08 ± 0.041
60	9.288+09 ± 0.033	3.700+08 ± 0.056
61	3.788+10 ± 0.025	1.957+09 ± 0.036
62	2.765+10 ± 0.025	1.605+09 ± 0.036
63	1.872+10 ± 0.035	1.594+09 ± 0.043
64	2.696+10 ± 0.023	1.747+09 ± 0.036
65	3.935+10 ± 0.027	1.771+09 ± 0.032
66	3.216+10 ± 0.029	1.458+09 ± 0.036
67	2.239+10 ± 0.028	1.590+09 ± 0.045
68	3.109+10 ± 0.025	1.935+09 ± 0.036

[a]A factor of 4π has already been included in these values.
[b]Read as 1.135×10^{10}.
[c]Fractional Standard Deviation.

Table 8

Neutron and Gamma Dose Levels in the SBI Platform from the Fission Sources Positioned Directly Above the Platform Body (rads·m²/kTon)[a]

	Neutron	Secondary Gamma	Prompt Gamma
1	1.622+07[b] ± 0.038[c]	1.693+07 ± 0.086	2.323+08 ± 0.034
2	1.683+07 ± 0.035	1.908+07 ± 0.117	2.762+08 ± 0.050
3	1.530+07 ± 0.028	1.705+07 ± 0.078	2.357+08 ± 0.035
4	1.332+07 ± 0.037	1.706+07 ± 0.065	1.969+08 ± 0.044
5	2.173+07 ± 0.028	1.988+07 ± 0.058	3.852+08 ± 0.038
6	2.020+07 ± 0.024	2.155+07 ± 0.068	3.577+08 ± 0.025
7	1.687+07 ± 0.030	2.080+07 ± 0.070	3.027+08 ± 0.041
8	1.867+07 ± 0.032	1.708+07 ± 0.061	3.537+08 ± 0.038
9	1.160+07 ± 0.025	1.483+07 ± 0.060	1.632+08 ± 0.034
10	1.191+07 ± 0.030	1.435+07 ± 0.072	1.737+08 ± 0.030
11	1.406+07 ± 0.032	1.785+07 ± 0.072	2.353+08 ± 0.044
12	3.337+07 ± 0.026	2.150+07 ± 0.052	6.320+08 ± 0.029
13	2.450+07 ± 0.019	2.370+07 ± 0.066	4.674+08 ± 0.024
14	2.397+07 ± 0.021	2.311+07 ± 0.051	4.702+08 ± 0.023
15	2.563+07 ± 0.026	2.114+07 ± 0.055	4.770+08 ± 0.030
16	1.915+07 ± 0.028	1.999+07 ± 0.109	3.529+08 ± 0.025
17	1.182+07 ± 0.034	1.221+07 ± 0.086	2.251+08 ± 0.030
18	2.988+07 ± 0.022	2.385+07 ± 0.052	5.783+08 ± 0.027
19	2.288+07 ± 0.028	1.915+07 ± 0.100	4.832+08 ± 0.032
20	2.230+07 ± 0.027	1.764+07 ± 0.057	5.098+08 ± 0.029
21	1.800+07 ± 0.029	2.220+07 ± 0.065	3.575+08 ± 0.030
22	1.101+07 ± 0.034	1.560+07 ± 0.115	2.292+08 ± 0.038
23	2.949+07 ± 0.024	2.585+07 ± 0.051	5.636+08 ± 0.032
24	2.219+07 ± 0.028	2.225+07 ± 0.083	4.627+08 ± 0.032
25	2.231+07 ± 0.027	1.959+07 ± 0.073	4.740+08 ± 0.032
26	1.619+07 ± 0.022	1.805+07 ± 0.068	3.095+08 ± 0.026
27	9.615+06 ± 0.031	1.010+07 ± 0.064	1.712+08 ± 0.034
28	2.790+07 ± 0.019	2.440+07 ± 0.057	5.446+08 ± 0.024
29	2.049+07 ± 0.022	1.616+07 ± 0.050	4.370+08 ± 0.025
30	1.905+07 ± 0.025	1.544+07 ± 0.046	4.114+08 ± 0.024
31	1.684+07 ± 0.021	1.816+07 ± 0.052	3.010+08 ± 0.029
32	9.686+06 ± 0.032	1.166+07 ± 0.082	1.707+08 ± 0.033
33	2.820+07 ± 0.021	2.276+07 ± 0.045	5.266+08 ± 0.027
34	2.046+07 ± 0.024	1.735+07 ± 0.047	4.502+08 ± 0.027

Table 8 (Continued)

	Neutron	Secondary Gamma	Prompt Gamma
35	2.024+07 ± 0.023	1.591+07 ± 0.058	4.092+08 ± 0.026
36	4.341+05 ± 0.041	3.253+06 ± 0.049	9.931+06 ± 0.030
37	2.283+05 ± 0.049	7.196+05 ± 0.074	3.968+06 ± 0.052
38	2.433+05 ± 0.046	7.172+05 ± 0.149	3.812+06 ± 0.047
39	2.111+05 ± 0.038	5.367+05 ± 0.070	3.343+06 ± 0.041
40	1.391+05 ± 0.044	3.227+05 ± 0.095	1.931+06 ± 0.044
41	4.370+05 ± 0.040	3.445+06 ± 0.057	1.040+07 ± 0.030
42	2.415+05 ± 0.049	8.262+05 ± 0.072	4.097+06 ± 0.045
43	2.337+05 ± 0.045	7.316+05 ± 0.115	3.856+06 ± 0.038
44	2.139+05 ± 0.040	6.445+05 ± 0.084	3.370+06 ± 0.035
45	1.365+05 ± 0.042	3.171+05 ± 0.106	1.925+06 ± 0.036
46	1.193+08 ± 0.011	3.296+07 ± 0.065	2.739+09 ± 0.015
47	1.838+07 ± 0.028	1.185+07 ± 0.105	3.856+08 ± 0.030
48	1.492+07 ± 0.028	8.564+06 ± 0.113	3.208+08 ± 0.034
49	1.212+07 ± 0.030	5.906+06 ± 0.098	2.583+08 ± 0.032
50	7.344+06 ± 0.036	2.940+06 ± 0.102	1.859+08 ± 0.038
51	1.511+09 ± 0.023	5.048+07 ± 0.041	6.504+08 ± 0.021
52	9.057+08 ± 0.033	2.765+07 ± 0.044	3.655+08 ± 0.025
53	4.728+09 ± 0.015	7.303+07 ± 0.035	1.082+09 ± 0.016
54	3.269+09 ± 0.020	5.082+07 ± 0.036	8.789+08 ± 0.018
55	3.168+09 ± 0.016	4.942+07 ± 0.038	9.021+08 ± 0.018
56	1.562+09 ± 0.022	5.526+07 ± 0.036	6.334+08 ± 0.021
57	8.708+08 ± 0.029	3.039+07 ± 0.042	3.584+08 ± 0.027
58	4.787+09 ± 0.017	6.866+07 ± 0.031	1.103+09 ± 0.019
59	3.249+09 ± 0.020	4.986+07 ± 0.035	8.678+08 ± 0.018
60	3.212+09 ± 0.018	5.264+07 ± 0.031	8.636+08 ± 0.021
61	2.891+09 ± 0.019	1.379+08 ± 0.034	1.378+09 ± 0.016
62	2.820+09 ± 0.018	1.321+08 ± 0.025	1.373+09 ± 0.018
63	1.274+10 ± 0.010	3.504+08 ± 0.019	4.038+09 ± 0.011
64	1.258+10 ± 0.012	3.606+08 ± 0.018	4.066+09 ± 0.013
65	2.778+09 ± 0.020	1.363+08 ± 0.029	1.374+09 ± 0.018
66	2.807+09 ± 0.019	1.414+08 ± 0.032	1.429+09 ± 0.016
67	1.240+10 ± 0.010	3.602+08 ± 0.020	4.119+09 ± 0.012
68	1.253+10 ± 0.010	3.522+08 ± 0.017	4.067+09 ± 0.012

[a]A factor of 4π has already been included in these values.
[b]Read as 1.622×10^7.
[c]Fractional Standard Deviation.

Table 9

Neutron and Gamma Dose Levels in the SBI Platform from the Fission Sources Positioned Directly Above the Solar Panels (rads·m^2/kTon)[a]

	Neutron	Secondary Gamma	Prompt Gamma
1	3.708+05[b] ± 0.271[c]	4.500+05 ± 0.313	9.216+05 ± 0.326
2	6.265+05 ± 0.205	9.660+05 ± 0.275	1.850+06 ± 0.341
3	5.099+05 ± 0.237	1.762+06 ± 0.417	2.494+06 ± 0.238
4	4.376+05 ± 0.174	1.436+06 ± 0.684	2.550+06 ± 0.276
5	5.589+05 ± 0.155	5.801+05 ± 0.347	2.330+06 ± 0.275
6	5.626+05 ± 0.203	8.486+05 ± 0.392	1.895+06 ± 0.314
7	5.377+05 ± 0.214	4.263+05 ± 0.288	1.690+06 ± 0.367
8	6.302+05 ± 0.164	1.061+06 ± 0.313	2.819+06 ± 0.178
9	5.074+05 ± 0.187	6.160+05 ± 0.298	2.736+06 ± 0.229
10	3.327+05 ± 0.189	6.921+05 ± 0.282	2.412+06 ± 0.266
11	7.092+05 ± 0.144	6.637+05 ± 0.318	3.455+06 ± 0.184
12	6.483+05 ± 0.135	4.021+05 ± 0.290	3.615+06 ± 0.175
13	4.511+05 ± 0.196	5.589+05 ± 0.328	2.667+06 ± 0.324
14	4.932+05 ± 0.195	1.282+06 ± 0.284	2.630+06 ± 0.267
15	6.796+05 ± 0.141	7.752+05 ± 0.250	2.191+06 ± 0.242
16	1.751+05 ± 0.377	1.367+06 ± 0.754	1.723+06 ± 0.297
17	2.314+05 ± 0.283	8.754+05 ± 0.520	1.756+06 ± 0.247
18	1.790+05 ± 0.286	4.116+05 ± 0.355	1.139+06 ± 0.325
19	4.488+05 ± 0.212	2.855+05 ± 0.358	2.589+06 ± 0.223
20	2.979+05 ± 0.223	7.849+05 ± 0.317	2.856+06 ± 0.218
21	1.417+05 ± 0.333	3.418+05 ± 0.272	8.634+05 ± 0.349
22	1.954+05 ± 0.282	8.445+05 ± 0.314	1.222+06 ± 0.307
23	8.864+04 ± 0.295	9.122+05 ± 0.294	1.065+06 ± 0.329
24	3.388+05 ± 0.215	1.118+06 ± 0.342	2.952+06 ± 0.238
25	3.786+05 ± 0.217	7.903+05 ± 0.256	1.965+06 ± 0.260
26	1.095+05 ± 0.241	1.422+06 ± 0.603	1.075+06 ± 0.272
27	1.938+05 ± 0.206	4.078+05 ± 0.429	1.892+06 ± 0.261
28	1.128+05 ± 0.264	3.606+05 ± 0.359	1.177+06 ± 0.241
29	3.822+05 ± 0.195	4.583+05 ± 0.388	2.649+06 ± 0.223
30	2.221+05 ± 0.218	5.379+05 ± 0.225	2.186+06 ± 0.234
31	1.404+05 ± 0.256	4.748+05 ± 0.292	4.962+05 ± 0.358
32	2.784+05 ± 0.176	2.105+06 ± 0.793	1.928+06 ± 0.214
33	1.683+05 ± 0.244	9.225+05 ± 0.477	9.796+05 ± 0.274
34	2.397+05 ± 0.188	4.336+05 ± 0.279	1.227+06 ± 0.205

Table 9 (Continued)

	Neutron	Secondary Gamma	Prompt Gamma
35	3.148+05 ± 0.170	3.841+05 ± 0.307	1.553+06 ± 0.240
36	4.733+07 ± 0.004	9.458+05 ± 0.102	1.390+09 ± 0.004
37	1.230+07 ± 0.008	6.196+05 ± 0.082	1.276+08 ± 0.010
38	1.026+07 ± 0.009	4.648+05 ± 0.079	1.032+08 ± 0.013
39	7.491+06 ± 0.007	3.744+05 ± 0.100	7.945+07 ± 0.014
40	3.482+06 ± 0.010	1.572+05 ± 0.099	4.581+07 ± 0.021
41	4.718+07 ± 0.004	8.222+05 ± 0.094	1.395+09 ± 0.005
42	1.210+07 ± 0.008	5.861+05 ± 0.100	1.294+08 ± 0.010
43	1.030+07 ± 0.009	4.416+05 ± 0.076	1.029+08 ± 0.012
44	7.474+06 ± 0.008	3.718+05 ± 0.085	7.930+07 ± 0.011
45	3.429+06 ± 0.011	1.426+05 ± 0.124	4.528+07 ± 0.019
46	6.268+06 ± 0.064	1.727+06 ± 0.328	1.561+07 ± 0.105
47	2.044+06 ± 0.120	3.003+05 ± 0.415	5.280+06 ± 0.161
48	1.332+06 ± 0.130	4.753+05 ± 0.446	6.202+06 ± 0.134
49	9.378+05 ± 0.111	1.347+05 ± 0.352	5.547+06 ± 0.121
50	3.938+05 ± 0.128	1.042+05 ± 0.385	3.456+06 ± 0.105
51	4.029+07 ± 0.175	2.369+06 ± 0.320	1.689+06 ± 0.261
52	5.721+07 ± 0.152	3.052+06 ± 0.263	3.249+06 ± 0.192
53	5.805+07 ± 0.118	1.986+06 ± 0.224	1.703+06 ± 0.262
54	8.247+07 ± 0.103	2.206+06 ± 0.156	4.349+06 ± 0.175
55	8.274+07 ± 0.124	2.755+06 ± 0.145	3.232+06 ± 0.142
56	3.669+07 ± 0.202	2.488+06 ± 0.155	1.339+06 ± 0.255
57	6.606+07 ± 0.134	2.066+06 ± 0.152	4.125+06 ± 0.175
58	4.284+07 ± 0.161	1.746+06 ± 0.155	1.891+06 ± 0.255
59	9.544+07 ± 0.118	3.507+06 ± 0.408	4.015+06 ± 0.154
60	9.044+07 ± 0.125	2.068+06 ± 0.139	2.815+06 ± 0.173
61	1.788+08 ± 0.088	1.053+07 ± 0.156	2.662+07 ± 0.112
62	2.092+08 ± 0.104	1.080+07 ± 0.118	2.187+07 ± 0.108
63	2.110+08 ± 0.082	1.085+07 ± 0.112	1.198+07 ± 0.127
64	2.409+08 ± 0.077	1.268+07 ± 0.095	1.300+07 ± 0.136
65	2.065+08 ± 0.097	1.143+07 ± 0.150	2.608+07 ± 0.100
66	2.323+08 ± 0.093	1.166+07 ± 0.114	1.990+07 ± 0.118
67	2.174+08 ± 0.089	1.334+07 ± 0.095	1.071+07 ± 0.136
68	2.414+08 ± 0.090	1.187+07 ± 0.092	1.228+07 ± 0.120

[a]A factor of 4π has already been included in these values.
[b]Read as 3.708×10^5.
[c]Fractional Standard Deviation.

Table 10

Neutron and Gamma Dose Levels in the SBI Platform from the Fission Sources Positioned Directly in Front of the Platform Body (rads·m²/kTon)[a]

	Neutron	Secondary Gamma	Prompt Gamma
1	2.975+06[b] ± 0.041[c]	4.865+06 ± 0.088	7.371+07 ± 0.047
2	2.255+07 ± 0.019	8.216+06 ± 0.051	5.009+08 ± 0.021
3	2.160+07 ± 0.021	7.897+06 ± 0.057	4.537+08 ± 0.023
4	2.287+07 ± 0.019	8.762+06 ± 0.063	4.756+08 ± 0.026
5	2.233+07 ± 0.021	9.996+06 ± 0.064	4.818+08 ± 0.023
6	2.097+07 ± 0.016	8.177+06 ± 0.067	4.582+08 ± 0.026
7	2.353+07 ± 0.022	8.051+06 ± 0.064	5.010+08 ± 0.021
8	8.883+06 ± 0.023	5.335+06 ± 0.052	1.928+08 ± 0.026
9	8.907+06 ± 0.022	5.528+06 ± 0.055	1.962+08 ± 0.024
10	8.656+06 ± 0.022	5.640+06 ± 0.053	1.952+08 ± 0.024
11	8.398+06 ± 0.026	5.670+06 ± 0.062	2.007+08 ± 0.026
12	8.657+06 ± 0.026	5.839+06 ± 0.055	1.914+08 ± 0.032
13	8.444+06 ± 0.024	5.521+06 ± 0.061	1.824+08 ± 0.026
14	8.705+06 ± 0.023	5.982+06 ± 0.084	2.004+08 ± 0.029
15	8.677+06 ± 0.024	5.495+06 ± 0.055	1.951+08 ± 0.030
16	1.493+07 ± 0.022	1.131+07 ± 0.058	2.856+08 ± 0.027
17	1.361+07 ± 0.020	8.769+06 ± 0.062	2.819+08 ± 0.028
18	1.354+07 ± 0.023	8.892+06 ± 0.053	2.797+08 ± 0.027
19	1.355+07 ± 0.022	9.544+06 ± 0.080	2.780+08 ± 0.024
20	1.380+07 ± 0.024	9.298+06 ± 0.055	2.648+08 ± 0.031
21	3.182+05 ± 0.101	1.063+06 ± 0.140	1.675+07 ± 0.080
22	2.549+05 ± 0.136	6.083+05 ± 0.162	1.645+07 ± 0.083
23	2.880+05 ± 0.102	8.525+05 ± 0.151	1.468+07 ± 0.097
24	2.237+05 ± 0.138	6.463+05 ± 0.189	1.584+07 ± 0.092
25	2.041+05 ± 0.137	5.661+05 ± 0.127	1.512+07 ± 0.077
26	2.664+07 ± 0.014	1.290+07 ± 0.051	5.502+08 ± 0.017
27	2.541+07 ± 0.012	1.088+07 ± 0.042	5.211+08 ± 0.017
28	2.533+07 ± 0.014	1.081+07 ± 0.040	5.162+08 ± 0.015
29	2.526+07 ± 0.013	1.026+07 ± 0.041	5.337+08 ± 0.015
30	2.571+07 ± 0.014	1.066+07 ± 0.035	5.129+08 ± 0.016
31	3.011+05 ± 0.101	4.675+05 ± 0.121	1.927+07 ± 0.058
32	2.398+05 ± 0.100	7.996+05 ± 0.234	1.666+07 ± 0.067
33	2.177+05 ± 0.133	5.332+05 ± 0.140	1.562+07 ± 0.059
34	2.080+05 ± 0.115	5.068+05 ± 0.243	1.541+07 ± 0.071

Table 10 (Continued)

	Neutron	Secondary Gamma	Prompt Gamma
35	2.102+05 ± 0.116	4.639+05 ± 0.156	1.554+07 ± 0.065
36	7.341+04 ± 0.058	5.780+05 ± 0.064	1.855+06 ± 0.048
37	5.034+04 ± 0.063	1.640+05 ± 0.107	1.049+06 ± 0.078
38	5.142+04 ± 0.064	1.398+05 ± 0.136	9.729+05 ± 0.061
39	5.413+04 ± 0.048	1.359+05 ± 0.133	9.740+05 ± 0.068
40	4.124+04 ± 0.048	6.390+04 ± 0.139	4.999+05 ± 0.056
41	7.008+04 ± 0.055	6.351+05 ± 0.074	2.099+06 ± 0.049
42	4.264+04 ± 0.068	1.593+05 ± 0.100	8.729+05 ± 0.067
43	5.405+04 ± 0.058	1.569+05 ± 0.109	1.019+06 ± 0.062
44	5.543+04 ± 0.062	1.166+05 ± 0.094	9.216+05 ± 0.072
45	4.706+04 ± 0.045	6.987+04 ± 0.161	5.712+05 ± 0.076
46	1.507+06 ± 0.057	4.175+06 ± 0.083	1.634+07 ± 0.064
47	2.953+05 ± 0.116	8.353+05 ± 0.261	4.080+06 ± 0.097
48	2.634+05 ± 0.118	5.253+05 ± 0.191	3.915+06 ± 0.098
49	2.035+05 ± 0.173	3.259+05 ± 0.157	2.877+06 ± 0.102
50	9.669+04 ± 0.136	2.488+05 ± 0.173	1.339+06 ± 0.093
51	2.186+09 ± 0.011	2.781+07 ± 0.032	6.038+08 ± 0.014
52	1.864+09 ± 0.014	1.973+07 ± 0.041	5.600+08 ± 0.015
53	1.899+09 ± 0.014	1.816+07 ± 0.037	5.502+08 ± 0.015
54	1.932+09 ± 0.012	1.953+07 ± 0.032	5.697+08 ± 0.014
55	1.917+09 ± 0.015	1.938+07 ± 0.029	5.578+08 ± 0.017
56	2.410+08 ± 0.032	5.219+06 ± 0.066	1.425+08 ± 0.025
57	1.912+08 ± 0.043	4.061+06 ± 0.084	1.098+08 ± 0.030
58	1.855+08 ± 0.036	3.648+06 ± 0.069	1.011+08 ± 0.031
59	1.832+08 ± 0.028	4.044+06 ± 0.076	1.097+08 ± 0.027
60	1.907+08 ± 0.039	3.395+06 ± 0.067	1.053+08 ± 0.030
61	1.771+09 ± 0.015	7.870+07 ± 0.024	7.393+08 ± 0.022
62	1.758+09 ± 0.014	7.877+07 ± 0.023	7.961+08 ± 0.022
63	1.750+09 ± 0.017	7.522+07 ± 0.023	7.657+08 ± 0.023
64	1.800+09 ± 0.015	7.781+07 ± 0.020	7.817+08 ± 0.022
65	3.477+08 ± 0.031	1.616+07 ± 0.045	9.783+07 ± 0.039
66	3.352+08 ± 0.031	1.638+07 ± 0.049	9.983+07 ± 0.041
67	3.377+08 ± 0.035	1.414+07 ± 0.046	1.070+08 ± 0.038
68	3.493+08 ± 0.035	1.557+07 ± 0.078	9.701+07 ± 0.038

[a]A factor of 4π has already been included in these values.
[b]Read as 2.975×10^6.
[c]Fractional Standard Deviation.

Table 11

Neutron and Gamma Dose Levels in the SBI Platform from the Fission Sources Positioned Directly in Front of and Above the Platform Body (rads·m²/kTon)[a]

	Neutron	Secondary Gamma	Prompt Gamma
1	1.008+08[b] ± 0.024[c]	3.658+07 ± 0.101	1.892+09 ± 0.021
2	1.442+07 ± 0.033	1.555+07 ± 0.111	1.577+08 ± 0.046
3	8.522+06 ± 0.043	1.115+07 ± 0.091	7.612+07 ± 0.051
4	1.265+07 ± 0.033	1.309+07 ± 0.072	1.363+08 ± 0.047
5	1.656+07 ± 0.036	1.376+07 ± 0.107	2.201+08 ± 0.052
6	1.378+07 ± 0.031	1.268+07 ± 0.083	1.630+08 ± 0.036
7	1.695+07 ± 0.034	1.230+07 ± 0.097	2.387+08 ± 0.044
8	2.205+07 ± 0.029	1.432+07 ± 0.123	3.588+08 ± 0.035
9	1.519+07 ± 0.028	1.393+07 ± 0.132	2.260+08 ± 0.033
10	1.522+07 ± 0.031	9.925+06 ± 0.073	2.455+08 ± 0.030
11	2.237+07 ± 0.025	1.234+07 ± 0.071	3.489+08 ± 0.035
12	2.553+07 ± 0.025	1.187+07 ± 0.068	4.191+08 ± 0.031
13	2.678+07 ± 0.020	1.455+07 ± 0.069	4.871+08 ± 0.028
14	2.735+07 ± 0.020	1.485+07 ± 0.079	4.892+08 ± 0.028
15	2.640+07 ± 0.024	1.557+07 ± 0.058	4.381+08 ± 0.031
16	3.815+06 ± 0.057	8.816+06 ± 0.095	2.966+07 ± 0.063
17	5.187+06 ± 0.052	7.141+06 ± 0.100	3.626+07 ± 0.076
18	3.997+06 ± 0.061	8.637+06 ± 0.085	3.372+07 ± 0.071
19	5.166+06 ± 0.056	7.480+06 ± 0.093	4.151+07 ± 0.081
20	4.048+06 ± 0.051	7.654+06 ± 0.089	3.468+07 ± 0.077
21	3.080+06 ± 0.067	8.280+06 ± 0.082	2.926+07 ± 0.085
22	3.437+06 ± 0.061	7.349+06 ± 0.176	2.990+07 ± 0.080
23	4.057+06 ± 0.061	7.311+06 ± 0.087	3.429+07 ± 0.090
24	3.996+06 ± 0.053	6.612+06 ± 0.091	4.070+07 ± 0.068
25	3.813+06 ± 0.050	7.096+06 ± 0.103	3.198+07 ± 0.078
26	3.968+06 ± 0.045	6.699+06 ± 0.065	3.645+07 ± 0.056
27	5.720+06 ± 0.037	6.736+06 ± 0.087	5.397+07 ± 0.044
28	1.044+07 ± 0.031	7.710+06 ± 0.101	1.732+08 ± 0.035
29	4.433+06 ± 0.042	6.414+06 ± 0.074	4.391+07 ± 0.041
30	3.851+06 ± 0.048	6.456+06 ± 0.100	3.351+07 ± 0.060
31	3.410+06 ± 0.046	7.261+06 ± 0.118	2.365+07 ± 0.069
32	3.855+06 ± 0.048	5.346+06 ± 0.105	3.053+07 ± 0.067
33	1.042+07 ± 0.028	7.312+06 ± 0.075	1.699+08 ± 0.042
34	4.086+06 ± 0.047	5.849+06 ± 0.088	3.620+07 ± 0.063

Table 11 (Continued)

	Neutron	Secondary Gamma	Prompt Gamma
35	3.536+06 ± 0.043	5.529+06 ± 0.077	2.873+07 ± 0.057
36	4.733+05 ± 0.036	1.803+06 ± 0.088	5.471+06 ± 0.044
37	2.853+05 ± 0.037	4.391+05 ± 0.148	2.190+06 ± 0.056
38	2.885+05 ± 0.041	3.831+05 ± 0.179	1.841+06 ± 0.061
39	2.531+05 ± 0.041	3.507+05 ± 0.110	1.703+06 ± 0.061
40	1.638+05 ± 0.039	1.462+05 ± 0.111	9.665+05 ± 0.058
41	5.015+05 ± 0.042	1.585+06 ± 0.066	5.665+06 ± 0.037
42	2.814+05 ± 0.050	4.075+05 ± 0.157	2.475+06 ± 0.069
43	2.740+05 ± 0.042	3.547+05 ± 0.103	2.100+06 ± 0.058
44	2.604+05 ± 0.040	2.938+05 ± 0.109	1.755+06 ± 0.066
45	1.711+05 ± 0.039	1.923+05 ± 0.161	9.670+05 ± 0.058
46	1.171+08 ± 0.014	2.037+07 ± 0.075	2.584+09 ± 0.016
47	2.298+07 ± 0.029	1.049+07 ± 0.131	4.325+08 ± 0.035
48	1.914+07 ± 0.030	7.651+06 ± 0.109	3.602+08 ± 0.031
49	1.285+07 ± 0.028	5.130+06 ± 0.131	2.608+08 ± 0.028
50	5.581+06 ± 0.032	1.781+06 ± 0.109	1.229+08 ± 0.040
51	7.493+08 ± 0.033	2.891+07 ± 0.051	5.625+07 ± 0.050
52	9.117+08 ± 0.030	2.171+07 ± 0.057	7.340+07 ± 0.054
53	2.459+09 ± 0.018	3.124+07 ± 0.046	4.992+08 ± 0.024
54	7.791+08 ± 0.041	2.121+07 ± 0.059	7.799+07 ± 0.041
55	6.677+08 ± 0.035	2.193+07 ± 0.056	6.144+07 ± 0.046
56	7.602+08 ± 0.031	2.601+07 ± 0.066	6.389+07 ± 0.048
57	7.280+08 ± 0.034	1.816+07 ± 0.088	7.100+07 ± 0.051
58	1.875+09 ± 0.021	2.406+07 ± 0.040	3.444+08 ± 0.027
59	8.379+08 ± 0.029	2.091+07 ± 0.065	8.009+07 ± 0.044
60	7.719+08 ± 0.030	1.999+07 ± 0.065	6.085+07 ± 0.052
61	2.427+09 ± 0.022	1.174+08 ± 0.041	3.360+08 ± 0.033
62	1.805+09 ± 0.024	8.721+07 ± 0.040	2.040+08 ± 0.039
63	1.165+09 ± 0.028	7.877+07 ± 0.033	1.194+08 ± 0.037
64	1.803+09 ± 0.024	1.041+08 ± 0.034	2.595+08 ± 0.032
65	2.077+09 ± 0.022	9.302+07 ± 0.032	2.979+08 ± 0.030
66	1.723+09 ± 0.026	8.488+07 ± 0.039	2.235+08 ± 0.041
67	1.355+09 ± 0.029	8.069+07 ± 0.039	1.599+08 ± 0.040
68	1.971+09 ± 0.019	9.501+07 ± 0.031	2.849+08 ± 0.031

[a]A factor of 4π has already been included in these values.
[b]Read as 1.008×10^8.
[c]Fractional Standard Deviation.

Table 12

Neutron Damage Dose Levels in Silicon Components from the Fusion Source For All Three Scenarios (rads(Si)·m^2/kTon)[a]

	Top	Front	12:00 O'Clock High
1	1.063+08[b] ± 0.031[c]	2.574+07 ± 0.027	6.973+08 ± 0.017
2	1.240+08 ± 0.024	1.452+08 ± 0.020	6.256+07 ± 0.038
3	1.129+08 ± 0.024	1.342+08 ± 0.015	3.708+07 ± 0.039
4	9.866+07 ± 0.031	1.504+08 ± 0.017	5.417+07 ± 0.034
5	1.515+08 ± 0.026	1.483+08 ± 0.016	7.983+07 ± 0.033
6	1.348+08 ± 0.021	1.374+08 ± 0.019	7.119+07 ± 0.028
7	1.168+08 ± 0.027	1.458+08 ± 0.020	8.591+07 ± 0.035
8	1.488+08 ± 0.030	5.707+07 ± 0.021	1.361+08 ± 0.022
9	8.799+07 ± 0.023	6.077+07 ± 0.020	9.012+07 ± 0.023
10	8.679+07 ± 0.023	5.746+07 ± 0.020	9.373+07 ± 0.026
11	9.340+07 ± 0.029	5.817+07 ± 0.020	1.350+08 ± 0.025
12	1.977+08 ± 0.023	5.685+07 ± 0.021	1.429+08 ± 0.025
13	1.621+08 ± 0.020	5.927+07 ± 0.023	1.582+08 ± 0.017
14	1.551+08 ± 0.017	5.896+07 ± 0.023	1.607+08 ± 0.019
15	1.483+08 ± 0.024	5.782+07 ± 0.019	1.538+08 ± 0.023
16	1.396+08 ± 0.021	1.048+08 ± 0.020	2.127+07 ± 0.050
17	9.833+07 ± 0.027	1.012+08 ± 0.017	2.539+07 ± 0.049
18	1.784+08 ± 0.019	9.826+07 ± 0.018	1.973+07 ± 0.042
19	1.480+08 ± 0.022	1.001+08 ± 0.020	2.053+07 ± 0.060
20	1.508+08 ± 0.020	1.010+08 ± 0.021	1.896+07 ± 0.049
21	1.425+08 ± 0.027	7.281+06 ± 0.054	1.900+07 ± 0.058
22	9.968+07 ± 0.028	5.400+06 ± 0.069	2.160+07 ± 0.052
23	1.780+08 ± 0.021	5.685+06 ± 0.056	2.622+07 ± 0.051
24	1.506+08 ± 0.022	5.163+06 ± 0.073	2.237+07 ± 0.054
25	1.501+08 ± 0.025	5.274+06 ± 0.063	1.782+07 ± 0.050
26	1.256+08 ± 0.020	1.571+08 ± 0.012	2.083+07 ± 0.043
27	8.615+07 ± 0.022	1.568+08 ± 0.012	2.520+07 ± 0.036
28	1.663+08 ± 0.018	1.547+08 ± 0.010	6.038+07 ± 0.026
29	1.282+08 ± 0.019	1.527+08 ± 0.011	1.934+07 ± 0.046
30	1.315+08 ± 0.021	1.554+08 ± 0.011	1.568+07 ± 0.045
31	1.257+08 ± 0.019	6.233+06 ± 0.044	1.995+07 ± 0.041
32	8.048+07 ± 0.023	4.453+06 ± 0.055	1.914+07 ± 0.047
33	1.656+08 ± 0.020	5.081+06 ± 0.053	6.549+07 ± 0.026
34	1.365+08 ± 0.021	4.727+06 ± 0.060	2.079+07 ± 0.043
35	1.308+08 ± 0.018	4.908+06 ± 0.050	1.518+07 ± 0.041
46	7.612+08 ± 0.012	1.054+07 ± 0.045	7.253+08 ± 0.011
47	8.439+07 ± 0.025	2.037+06 ± 0.096	1.078+08 ± 0.027
48	7.331+07 ± 0.033	1.523+06 ± 0.100	8.500+07 ± 0.030
49	5.977+07 ± 0.027	1.230+06 ± 0.096	5.952+07 ± 0.026
50	4.299+07 ± 0.032	5.916+05 ± 0.103	2.527+07 ± 0.031

[a]A factor of 4π has already been included in these values.
[b]Read as 1.063×10^8.
[c]Fractional Standard Deviation.

Table 13

Neutron Damage Dose Levels in Silicon Components from the ^{235}U Fission Source For All Three Scenarios (rads(Si)·m^2/kTon)[a]

	Top	Front	12:00 O'Clock High
1	7.060+06[b] ± 0.038[c]	1.423+06 ± 0.041	4.168+07 ± 0.026
2	7.044+06 ± 0.035	9.376+06 ± 0.020	6.732+06 ± 0.034
3	6.623+06 ± 0.032	8.982+06 ± 0.022	4.165+06 ± 0.042
4	6.006+06 ± 0.039	9.574+06 ± 0.018	6.009+06 ± 0.034
5	9.377+06 ± 0.028	9.238+06 ± 0.021	7.552+06 ± 0.036
6	8.671+06 ± 0.026	8.777+06 ± 0.017	6.495+06 ± 0.031
7	7.446+06 ± 0.030	9.799+06 ± 0.024	7.837+06 ± 0.033
8	7.787+06 ± 0.029	3.793+06 ± 0.024	9.391+06 ± 0.030
9	4.993+06 ± 0.025	3.804+06 ± 0.024	6.711+06 ± 0.030
10	5.239+06 ± 0.031	3.652+06 ± 0.025	6.688+06 ± 0.033
11	6.174+06 ± 0.033	3.622+06 ± 0.027	9.649+06 ± 0.025
12	1.406+07 ± 0.029	3.690+06 ± 0.028	1.101+07 ± 0.025
13	1.044+07 ± 0.020	3.537+06 ± 0.024	1.158+07 ± 0.022
14	1.020+07 ± 0.022	3.645+06 ± 0.025	1.206+07 ± 0.021
15	1.109+07 ± 0.028	3.699+06 ± 0.025	1.146+07 ± 0.025
16	8.021+06 ± 0.030	6.046+06 ± 0.022	1.923+06 ± 0.057
17	4.839+06 ± 0.036	5.501+06 ± 0.021	2.513+06 ± 0.052
18	1.274+07 ± 0.024	5.477+06 ± 0.025	1.932+06 ± 0.062
19	9.878+06 ± 0.030	5.505+06 ± 0.022	2.409+06 ± 0.055
20	9.408+06 ± 0.028	5.597+06 ± 0.024	1.958+06 ± 0.051
21	7.559+06 ± 0.031	1.284+05 ± 0.096	1.529+06 ± 0.066
22	4.689+06 ± 0.036	1.038+05 ± 0.116	1.681+06 ± 0.061
23	1.252+07 ± 0.027	1.147+05 ± 0.112	1.999+06 ± 0.059
24	9.316+06 ± 0.030	9.626+04 ± 0.125	1.955+06 ± 0.053
25	9.622+06 ± 0.029	9.307+04 ± 0.144	1.864+06 ± 0.050
26	6.777+06 ± 0.025	1.114+07 ± 0.016	1.917+06 ± 0.045
27	4.126+06 ± 0.034	1.054+07 ± 0.014	2.751+06 ± 0.036
28	1.175+07 ± 0.021	1.054+07 ± 0.015	4.562+06 ± 0.031
29	8.732+06 ± 0.022	1.043+07 ± 0.015	2.123+06 ± 0.040
30	7.999+06 ± 0.026	1.067+07 ± 0.015	1.858+06 ± 0.047
31	7.246+06 ± 0.025	1.140+05 ± 0.096	1.705+06 ± 0.047
32	4.190+06 ± 0.034	9.488+04 ± 0.093	1.828+06 ± 0.047
33	1.209+07 ± 0.023	8.452+04 ± 0.137	4.596+06 ± 0.030
34	8.689+06 ± 0.026	8.507+04 ± 0.120	1.946+06 ± 0.049
35	8.614+06 ± 0.024	9.076+04 ± 0.109	1.731+06 ± 0.044
46	4.851+07 ± 0.012	6.983+05 ± 0.058	4.725+07 ± 0.016
47	8.042+06 ± 0.029	1.443+05 ± 0.116	1.005+07 ± 0.032
48	6.542+06 ± 0.029	1.267+05 ± 0.120	8.417+06 ± 0.031
49	5.251+06 ± 0.031	9.966+04 ± 0.169	5.726+06 ± 0.029
50	3.018+06 ± 0.037	4.596+04 ± 0.139	2.471+06 ± 0.032

[a] A factor of 4π has already been included in these values.
[b] Read as 7.060×10^6.
[c] Fractional Standard Deviation.

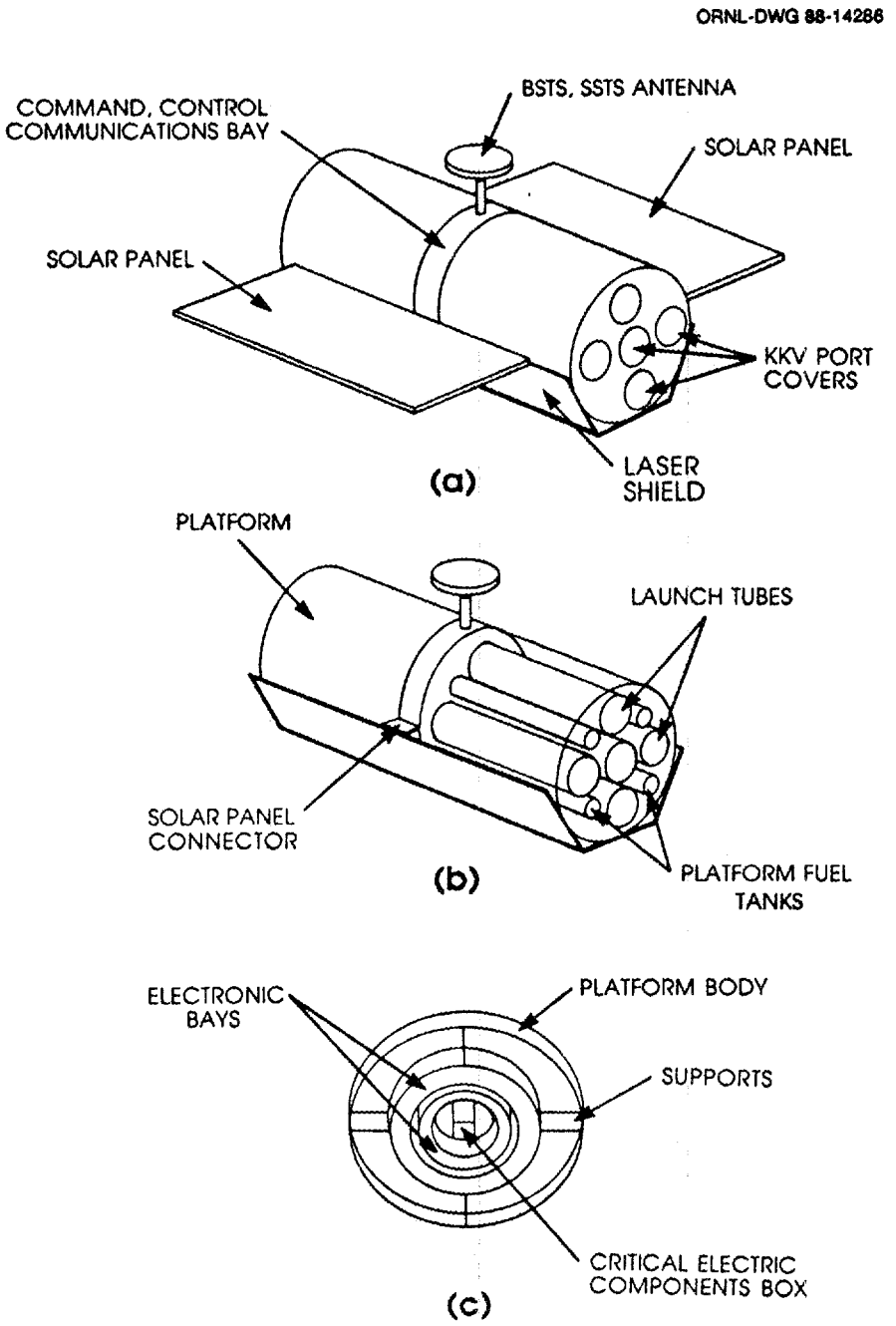

Figure 1. Calculational Model of the Space Based Interceptor Weapon Platform (a), with Interior Views Showing Launch Tube-Fuel Tanks Cluster (b), and the Central C^3 Bay (c).

ORNL-DWG 88-14287

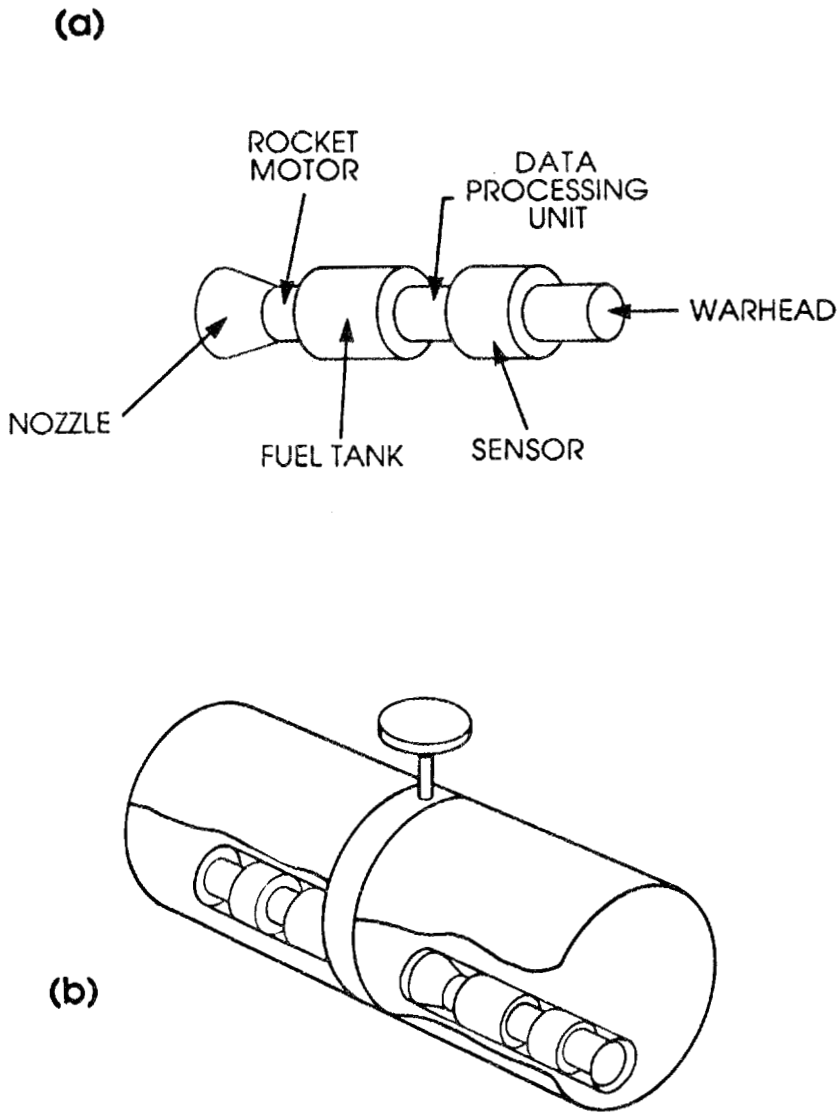

Figure 2. Kinetic Kill Vehicle (a) and Exploded View of SBI Weapon Platform Showing KKVs Inside Launch Tubes (b).

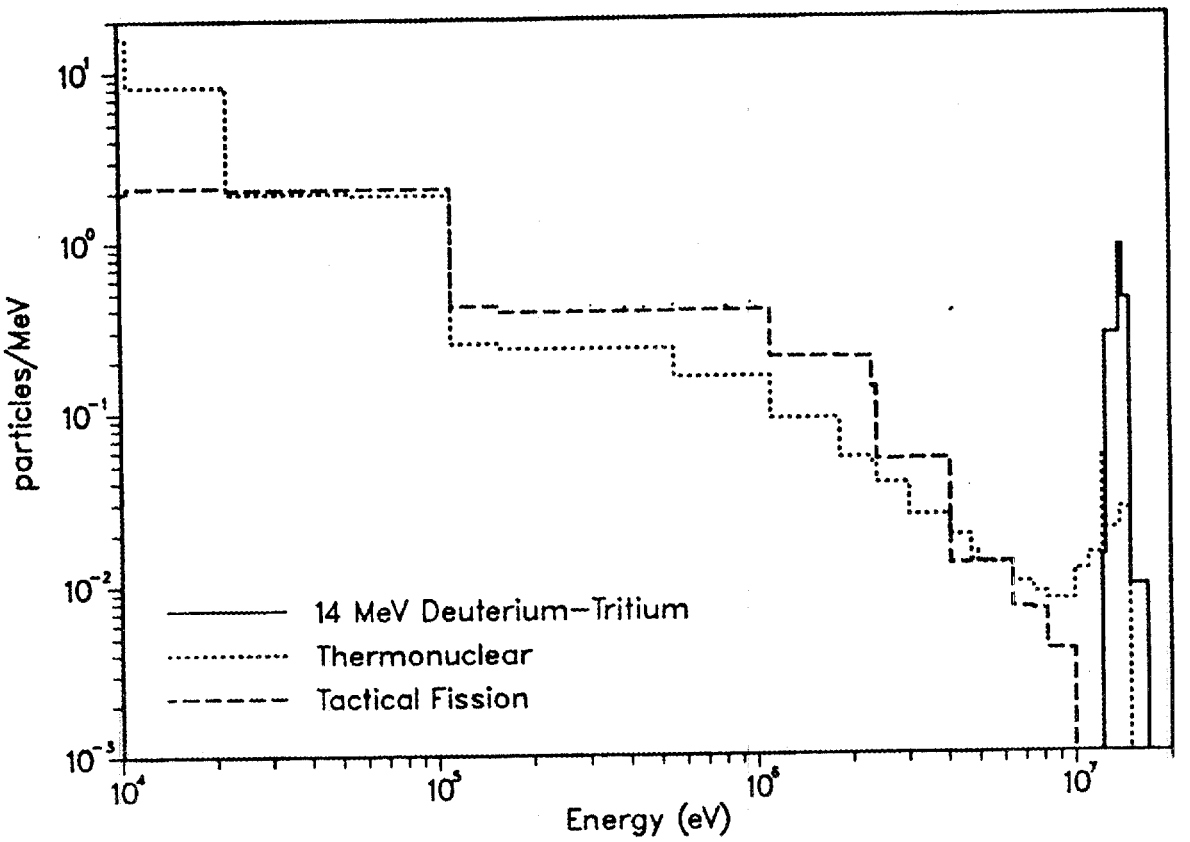

Figure 3. DABL Unclassified Neutron Source Spectra.

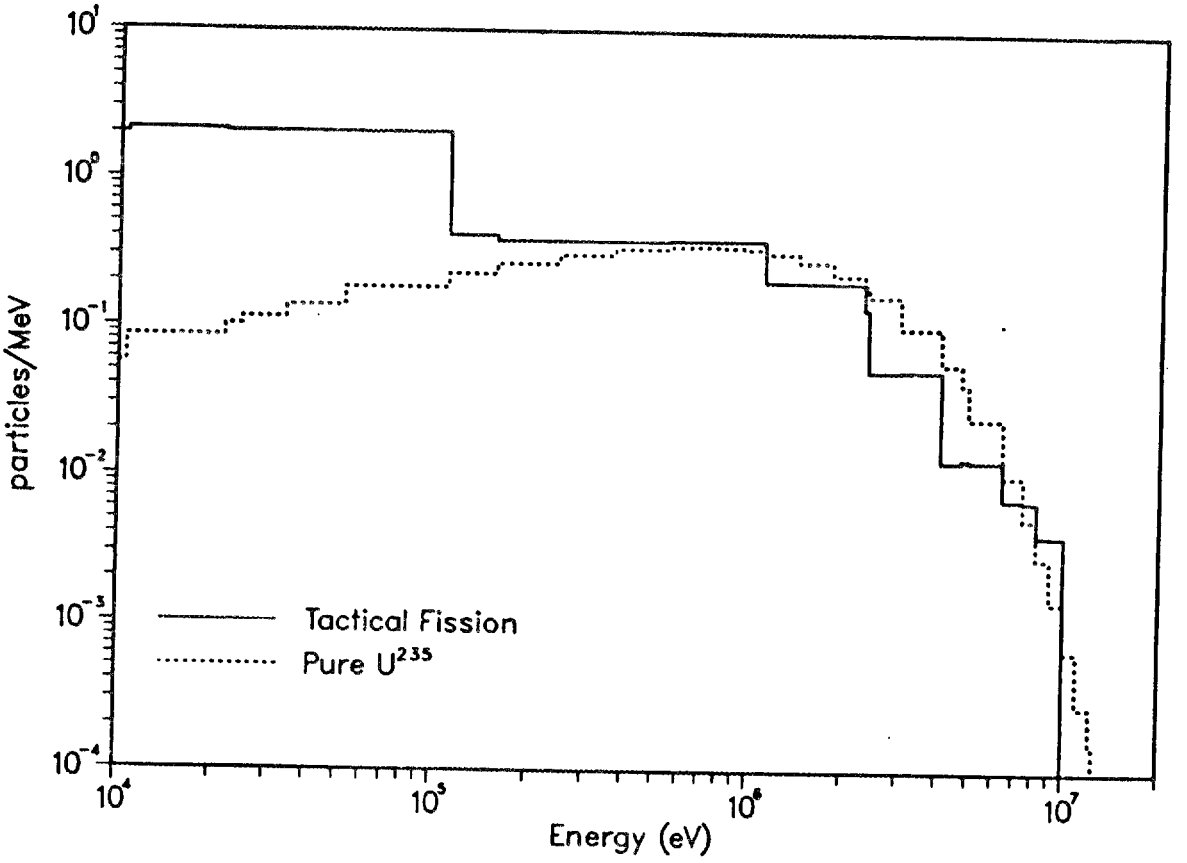

Figure 4. Normalized Fission Neutron Source Spectra.

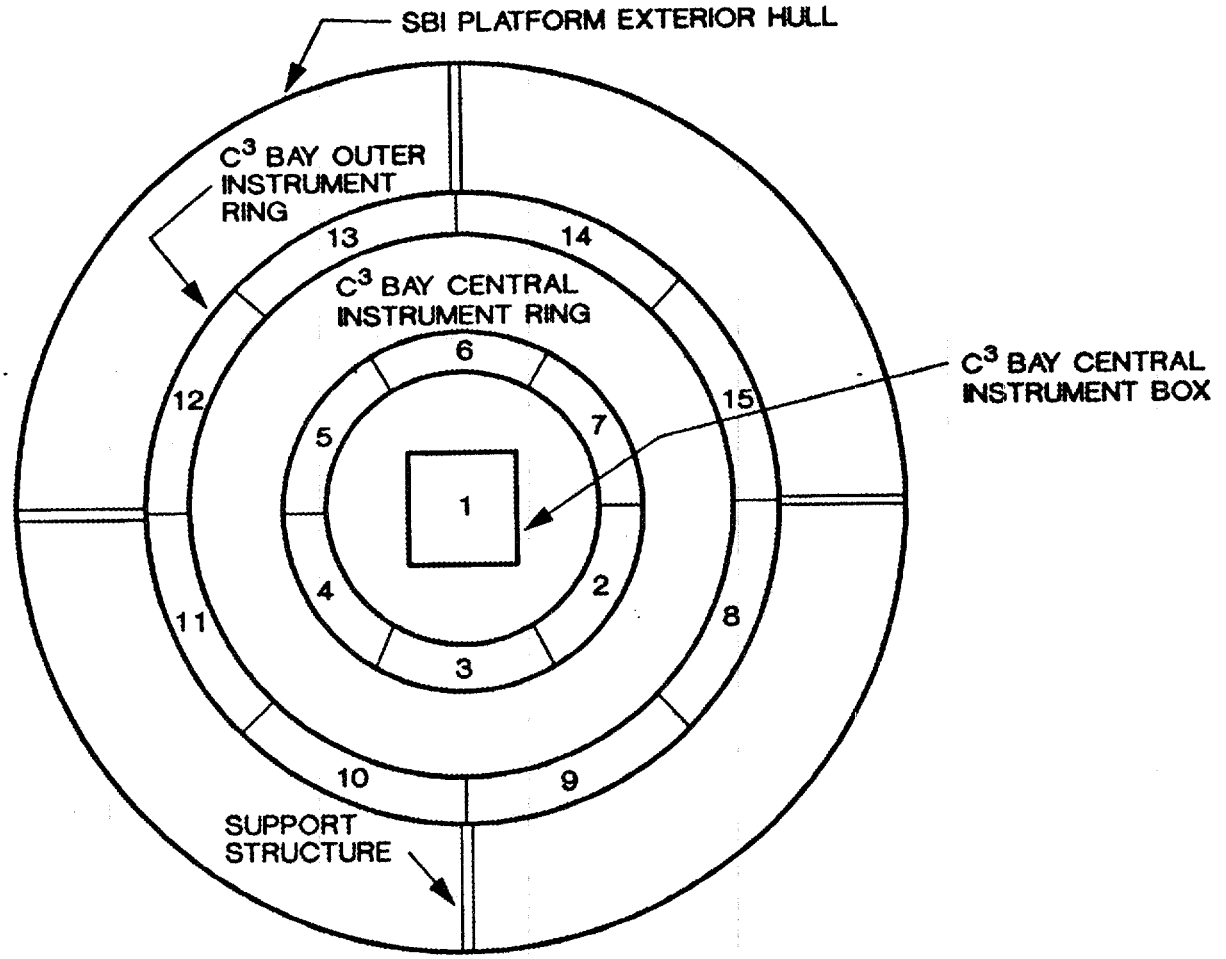

Figure 5. Schematic diagram of the Space Based Interceptor Weapon Platform Command, Control, Communications (C^3) Bay detailing the detector region numbering system used in the radiation transport analysis.

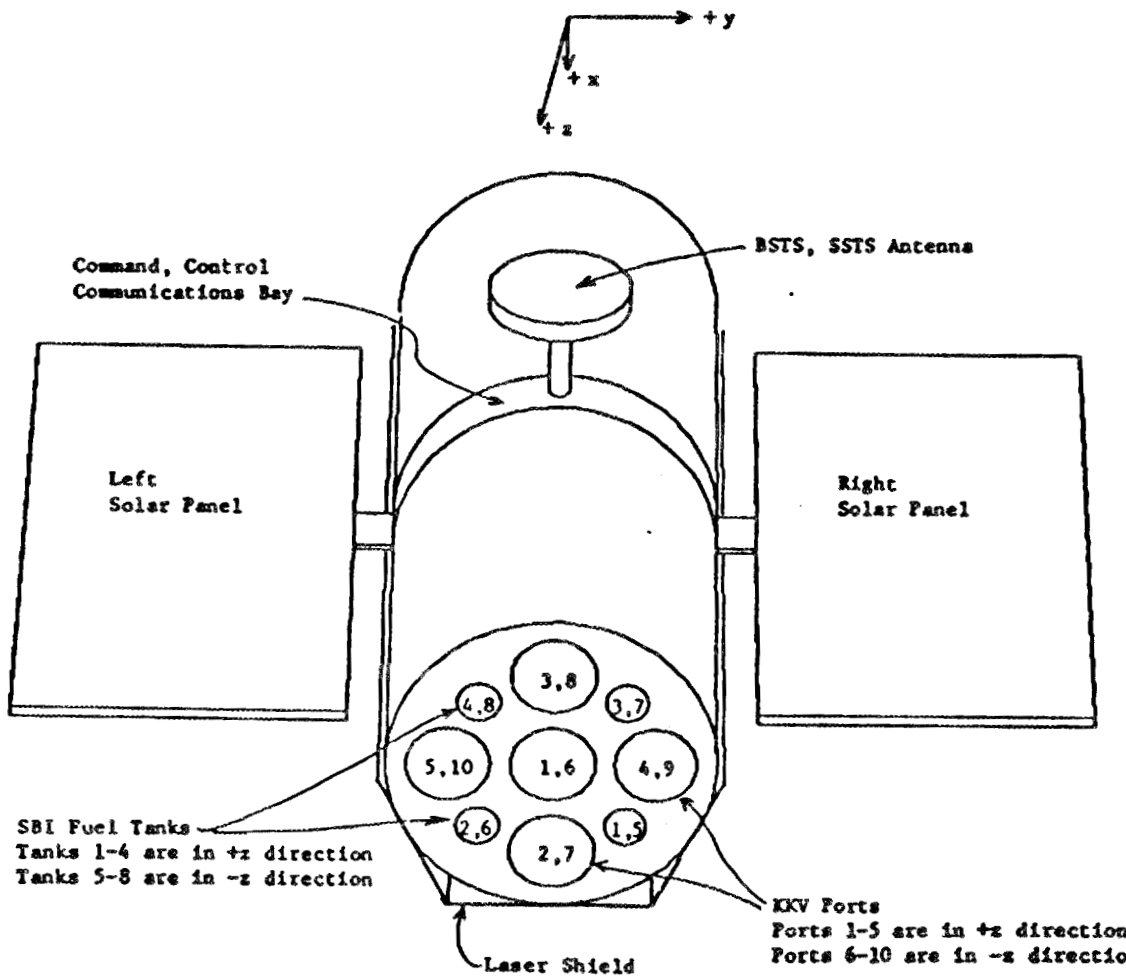

Figure 6. Schematic diagram of the Space Based Interceptor Weapon Platform detailing the kinetic kill vehicle and fuel tank numbering system used in the radiation transport analysis.

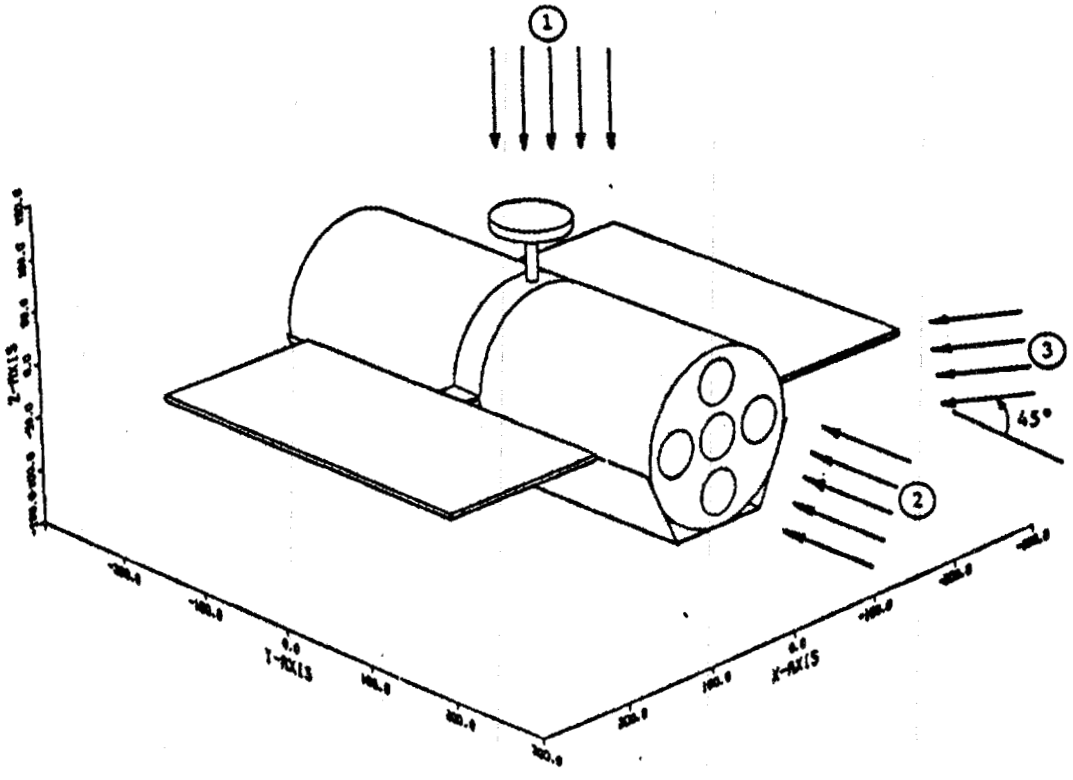

1 Incident on Top of SBI Platform

2 Incident on Front of SBI Platform

3 Incident on Front and Top at 45° Angle

Figure 7. Schematic diagram of the Space Based Interceptor Weapon Platform depicting directions of incident nuclear weapon source spectra.

REFERENCES

1. L. W. Ricketts, "Fundamentals of Nuclear Hardening of Electronic Equipment," Wiley–Interscience, New York, NY, 1972.
2. R. T. Santoro and T. A. Gabriel, "Shield Optimization Program, Part I: Executive Summary," Oak Ridge National Laboratory, Oak Ridge, Tennessee.
3. J. M. Barnes, R. T. Santoro, J. O. Johnson, J. D. Drischler, T. A. Gabriel, and M. S. Smith, "Shield Optimization Program, Part II: Effects of Van Allen Belt Radiation on SDI Weapon Platforms," ORNL/TM-10957, Oak Ridge National Laboratory, Oak Ridge, Tennessee.
4. J. O. Johnson, T. A. Gabriel, J. M. Barnes, J. D. Drischler, M. S. Smith, and R. T. Santoro, "Shield Optimization Program, Part III: Effects of X-Ray Radiation From Nuclear Weapons on SDI Weapon Platforms," ORNL/TM-10985, Oak Ridge National Laboratory, Oak Ridge, Tennessee.
5. M. S. Smith, T. J. Burns, J. O. Johnson, J. M. Barnes, J. D. Drischler, T. A. Gabriel, and R. T. Santoro, "Shield Optimization Program, Part V: A Hydrodynamic Comparison Using HULL and PUFF-TFT for a One-Dimensional Aluminum Slab," Oak Ridge National Laboratory, Oak Ridge, Tennessee.
6. M. S. Smith, S. McNeany, R. T. Santoro, and T. A. Gabriel, "Shield Optimization Program, Part VI: The Effect of Impurity Layers on the Hydrodynamic Response of a Beryllium Target to Mono-Energetic X-Rays Using the PUFF-TFT Code," ORNL/TM-11038, Oak Ridge National Laboratory, Oak Ridge, Tennessee.
7. D. T. Ingersoll, R. W. Roussin, C. Y. Fu, and J. E. White, "DABL69: A Broad–Group Neutron/Photon Cross–Section Library for Defense Nuclear Applications," ORNL/TM–10568, Oak Ridge National Laboratory, (in press).
8. B. E. Watt, "Energy Spectrum of Neutrons from Thermal Fission of ^{235}U," Phys. Rev. **87**, 1037 (1952).
9. M. B. Emmett, "The MORSE Monte Carlo Radiation Transport Code System," ORNL/TM–4972/R2, Oak Ridge National Laboratory, (July 1984).
10. T. A. Gabriel, J. M. Barnes, B. L. Bishop, J. D. Drishler, J. O. Johnson, R. A. Lillie, R. T. Santoro, and M. S. Smith, "The Oak Ridge National Laboratory Strategic Defense Initiative Shield Optimization Program", ORNL/TM–10631, Oak Ridge National Laboratory, (April 1988).

INTERNAL DISTRIBUTION

1. R. G. Alsmiller, Jr.
2. B. R. Appleton
3. D. E. Bartine
4–8. J. M. Barnes
9. T. J. Burns
10. R. M. Davis
11. J. B. Dooley
12–16. J. D. Drischler
17–21. T. A. Gabriel
22. C. M. Haaland
23. E. B. Harris
24. D. T. Ingersoll
25–29. J. O. Johnson
30. R. A. Lillie
31. F. C. Maienschein
32. J. R. Merriman
33. W. L. Roberts
34. R. W. Roussin
35–39. R. T. Santoro
40–44. M. S. Smith
45. D. G. Thomas
46. R. C. Ward
47. C. R. Weisbin
48. EPMD Reports Office
49–50. Laboratory Records Department
51. Laboratory Records, ORNL-RC
52. Document Reference Section
53. Central Research Library
54. ORNL Patent Section

EXTERNAL DISTRIBUTION

55. Dr. Charles Aeby, AFWL/NTC, Air Force Weapons Laboratory, Kirtland Air Force Base, New Mexico 87117-6008
56. Lt Dale Atkinson, AFWL/NTCA, Air Force Weapons Laboratory, Kirtland Air Force Base, New Mexico 87117-6008
57. J. J. Dorning, Department of Nuclear Engineering and Engineering Physics, Thornton Hall, University of Virginia, Charlottesville, Virginia 22901
58. Lt Richard Engstrom, AFWL/NTCA, Air Force Weapons Laboratory, Kirtland Air Force Base, Albuquerque, New Mexico 87117
59. R. M. Haralick, Department of Electrical Engineering, University of Washington, Seattle, Washington 98195
60. Office of the Assistant Manager for Energy Research and Development, Department of Energy, Oak Ridge Operations, P.O. Box 2001, Oak Ridge, TN 37831

61–70. Office of Scientific and Technical Information, P.O. Box 62, Oak Ridge, Tennessee 37830